

~~GEAT 3~~

Watkins, JS, and Drake, 1983
Studies in Continental Margin Geology
AAPG Memoir 34
29/83

Growth Faulting and Salt Diapirism: Their Relationship and Control in the Carolina Trough, Eastern North America

William P. Dillon
Peter Popenoe
John A. Grow
Kim D. Klitgord

B. Ann Swift
Charles K. Paul
Katharine V. Cashman

*U.S. Geological Survey
Woods Hole, Massachusetts*

The Carolina Trough is a long, linear, continental margin basin off eastern North America. Salt domes along the trough's seaward side show evidence of active diapirism and a normal growth fault along its landward side has been continually active at least since the end of the Jurassic. This steep fault extends to a strong reflection event at about 11 km depth that may represent the top of a salt layer. We infer that faulting is caused by seaward flow of salt from the deep part of the trough into domes, thereby removing support for the overlying block of sedimentary rock. Diapirs off eastern North America seem to be concentrated in the Carolina Trough and Scotian Basin, where basement seems to be thinner than in other basins off eastern North America, south of Newfoundland. Thinner basement, probably due to greater stretching during rifting, may have resulted in earlier subsidence below sea level, a longer life for the salt evaporating pans in these basins, and thus a thicker salt layer, which would be more conducive to diapirism.

The Carolina Trough is one of the four major basins off the United States' east coast, and it is unusual in its configuration and its history of postrift faulting and diapirism. This paper considers the causes of this faulting, the relationship of faulting to salt diapirism, and the reasons for localization of these processes on the eastern North American continental margin.

The Carolina Trough (Figure 1) is long, narrow, and linear, unlike the other east coast basins. It is about 450 km long and 40 km wide and also unlike the other basins, it does not seem to be segmented along the extensions of oceanic fracture zones, although it is terminated by such features. This effect is most notable at its southern end (Figure 1), where the extension of the Blake Spur Fracture Zone abruptly separates the Carolina Trough from the Blake Plateau Basin to the south.

A major system of normal faults extends for more than 300 km along the northwestern (landward) side of the basin and a linear group of diapirs is located on the basin's southeastern side (Figure 1). The diapirs are considered to be cored by salt because the chlorinity values distinctly increase downward in short sediment cores taken on top of them (F. T. Manheim, unpublished data, 1980). Distribution of the diapirs indicated in Figure 1 is based on the grid of multi-

channel seismic profiles shown, plus a much denser grid of single-channel seismic lines and a long-range sidescan-sonar survey. Sidescan-sonar was useful because many diapirs disrupt the sea floor.

EVIDENCE FOR MAJOR GROWTH FAULTING AND DIAPIRISM

To examine the structure of the Carolina Trough, we consider three adjacent multichannel seismic lines: BT1, 32, and TD6 (locations shown in Figure 1). These three profiles cross the central part of the trough and are about 60 km apart.

Seismic profile BT1

A part of profile BT1, showing a complete crossing of the trough, is presented in Figure 2 and its interpretation is shown in Figure 3. We interpret that an unconformity, giving rise to diffractions, dips to the southeast at the left side of the profile segment and extends beneath a set of very strong subhorizontal reflectors at 6 to 7 seconds. The unconformity is considered to be the postrift unconformity or breakup unconformity (Falvey, 1974), and the strong subhorizontal reflections are considered to arise from salt

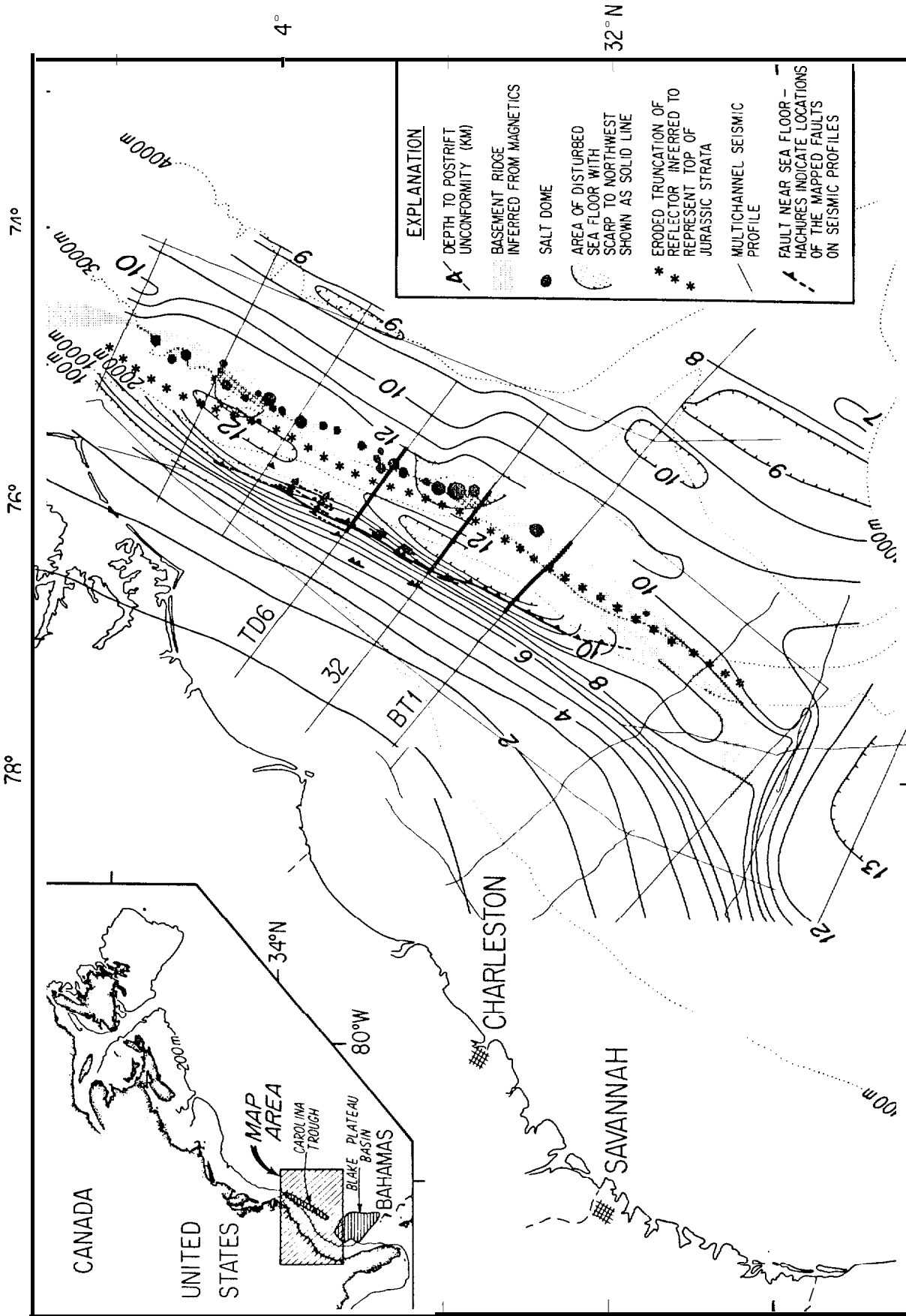


Figure 1 — The Carolina Trough. Contours showing depth in kilometers to the postrift unconformity are based on multichannel seismic-reflection profiles. The difficulty in defining this horizon is discussed in the text. Near-surface locations of faults are mapped. Locations of faults and diapirs are based on multichannel seismic profiles (locations shown), a much more dense coverage of single-channel seismic profiles and, for the diapirs, a single *Gloria* sidescan swath run along the axis of the group of diapirs. Hachures on faults show downthrown side and also indicate location of a profile crossing the fault. Lightly dotted lines are bathymetric contours. The parts of the three seismic lines shown in Figures 2, 7, and 11 are thickened.

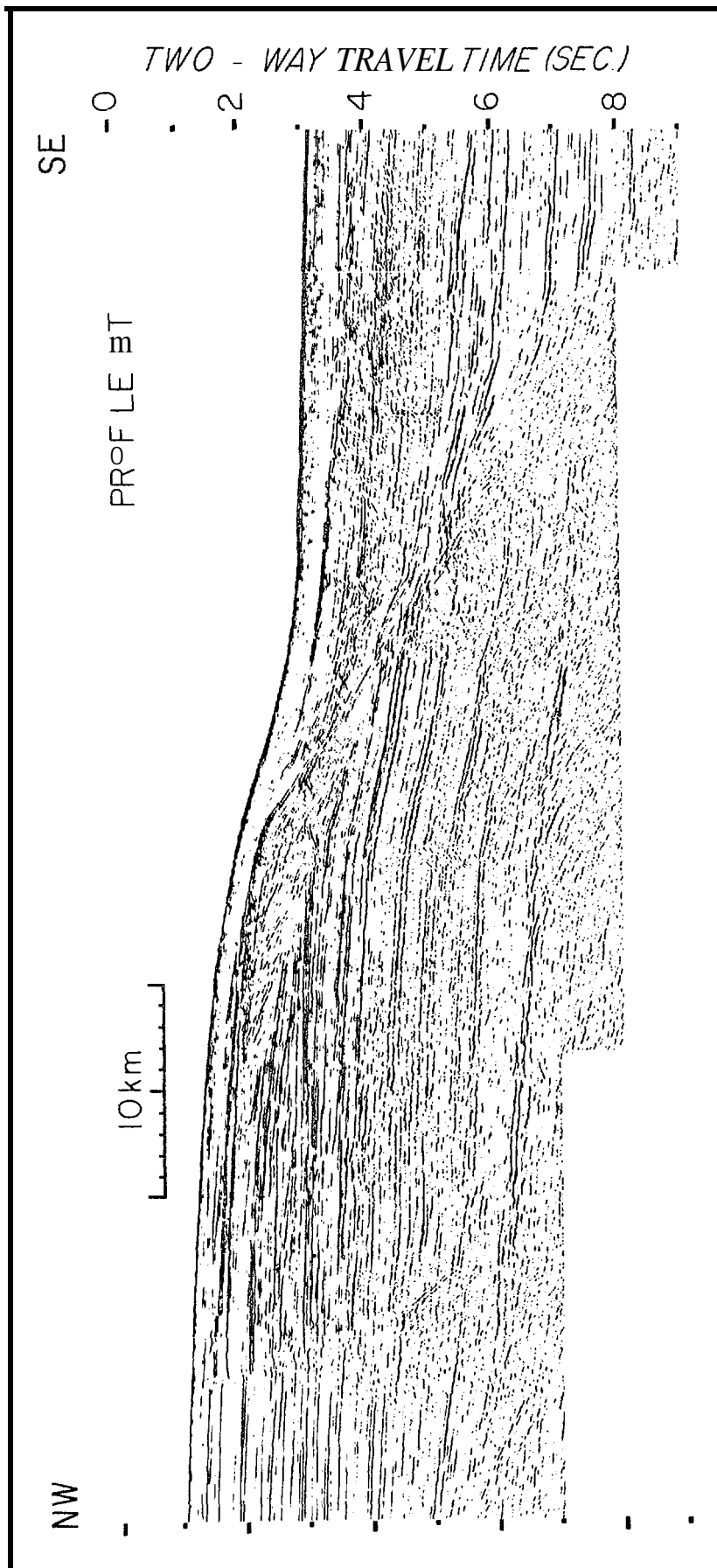


Figure 2 — Part of seismic profile BT1 that crosses the Carolina Trough (northwest is to left). Profile location is shown in Figure 1. Data were collected by Geophysical Service Incorporated (GSI) using a 1310-cu in (21,467 cu cm) airgun array, and a 48-trace, 3600-m streamer. Data were processed by GSI for a 36-fold stack. The strong set of reflections at 6 to 7 seconds to the left of center may arise from a salt layer. The bottom simulating reflector (BSR) at 0.3 to 0.5 seconds subbottom depth in the middle and right side of the figure probably represents the base of gas hydrate cementation of sediment (Dillon, Grow, and Pauli, 1980; Pauli and Dillon, 1981). No reflections indicative of major reef development are apparent in this profile.

(although they are marked in the interpretations with reversed L's for salt and rhombs to signify the possibility of a dolomite layer, which also could produce a strong reflection).

The postrift or breakup unconformity originally was defined as forming by erosion during a postulated "final uplift pulse associated with pre-breakup upwelling in the mantle," representing "the youngest cycle of subaerial erosion in a marginal basin." It was thought to be "very nearly the same age as the oldest oceanic crust in the adjacent deep ocean basin" (Falvey, 1974). The emphasis on subaerial erosion was Falvey's.

The reflection event that we called the postrift unconformity is mapped in Figure 1 to define the trough. The postrift unconformity is definable without controversy northwest of the inferred salt pinchout (Figure 2), where it is considered an eroded surface on Paleozoic basement and early Mesozoic continental deposits. To best define the Carolina Trough, we contoured the extension of this surface, atop Paleozoic and early Mesozoic rocks, where it continues southeastward beneath the inferred salt in the deepest part of the trough. It is unclear whether this horizon is truly the postrift unconformity because we do not know the relative age of the salt. Did seawater find its way into the trough during the rifting stage, resulting in the salt forming as a synrift deposit? In that case, the post-rift unconformity should be extended across the top of the salt. Alternatively, did the salt form just after the rift to drift change? At that time newly formed oceanic crust might have floated deep

isostatically and formed a channelway, allowing oceanic water to finally enter the trough. In the latter case, the post-rift unconformity would occur beneath the inferred salt, if it existed at all. A subaerially eroded post-rift "unconformity would not exist in the deepest part of the trough if deposition had been continuous there after initial subsidence in the rifting stage. The problem of the nature and location of the postrift unconformity in the Carolina Trough is unsolvable at present.

The unconformity is identified with difficulty seaward of the pinchout of the strong "salt" reflector, and contours are dropped where identification becomes too extremely imaginative. Much of the obscuring of basement seems due to diffractions arising at the eroded paleoslope formed of truncated Jurassic and Cretaceous strata. Some interpreters of magnetic data place a magnetic basement ridge in this region of obscured seismic returns (Klitgord and Behrendt, 1979), whereas others model no such ridge (Hutchinson and others, this volume). If no ridge is modeled, the magnetic anomaly is considered to be due to the contact of basements of different magnetic susceptibilities. We avoided the controversy by simply indicating the location of the proposed ridge (Klitgord and Behrendt, 1979) with a dot pattern (Figure 1). The point is significant because the diapirs are aligned on the magnetic anomaly that can be modeled as a ridge, and the possibility of control of diapir location by basement structure should be considered.

Several faults are indicated in Figure 3. The dominant fault, shown on the left of the figure, is observ-

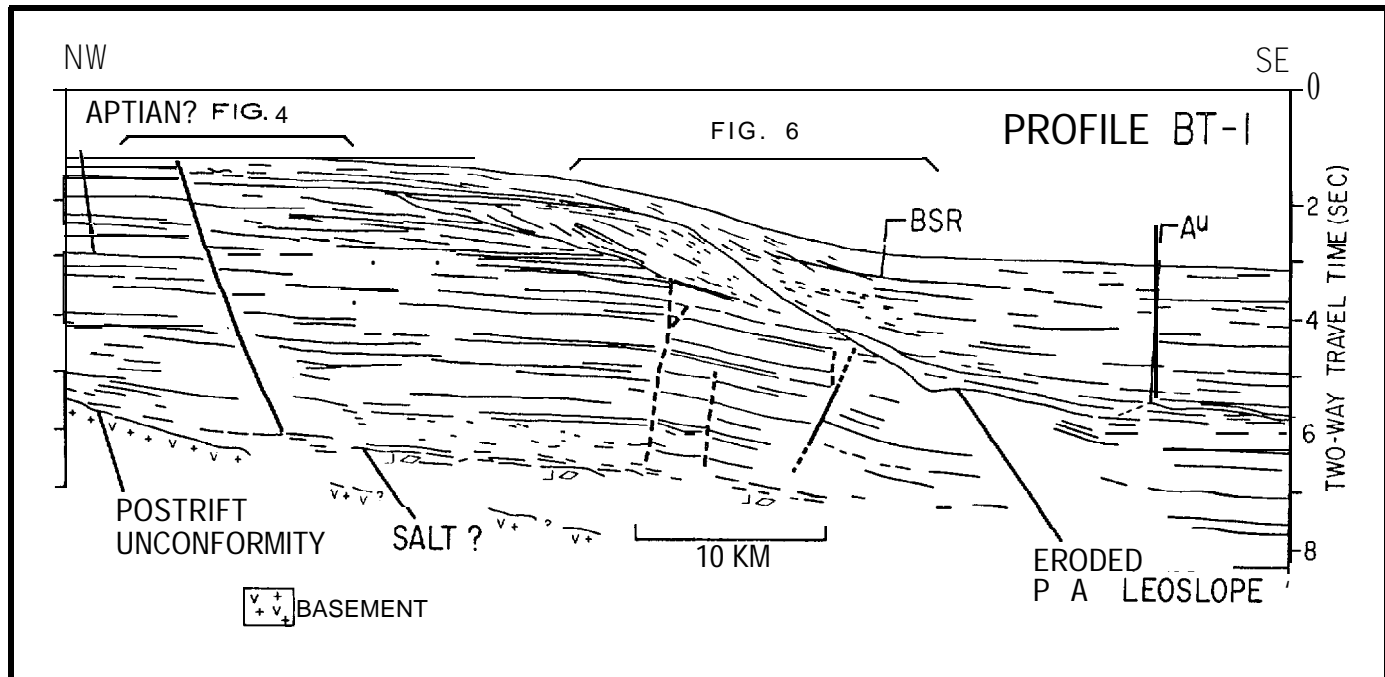


Figure 3 — Interpretation of the section of seismic profile BT1 shown in Figure 2. Light lines indicate reflections, heavy lines show interpreted faults. Brackets show location of detailed record photos shown in Figures 4 and 6. Stratigraphic identifications in this and other profile interpretations (Figures 8 and 12) are based on long-distance extrapolation from drilled horizons and should be considered preliminary BSR, bottom simulating reflector; Au, horizon A unconformity.

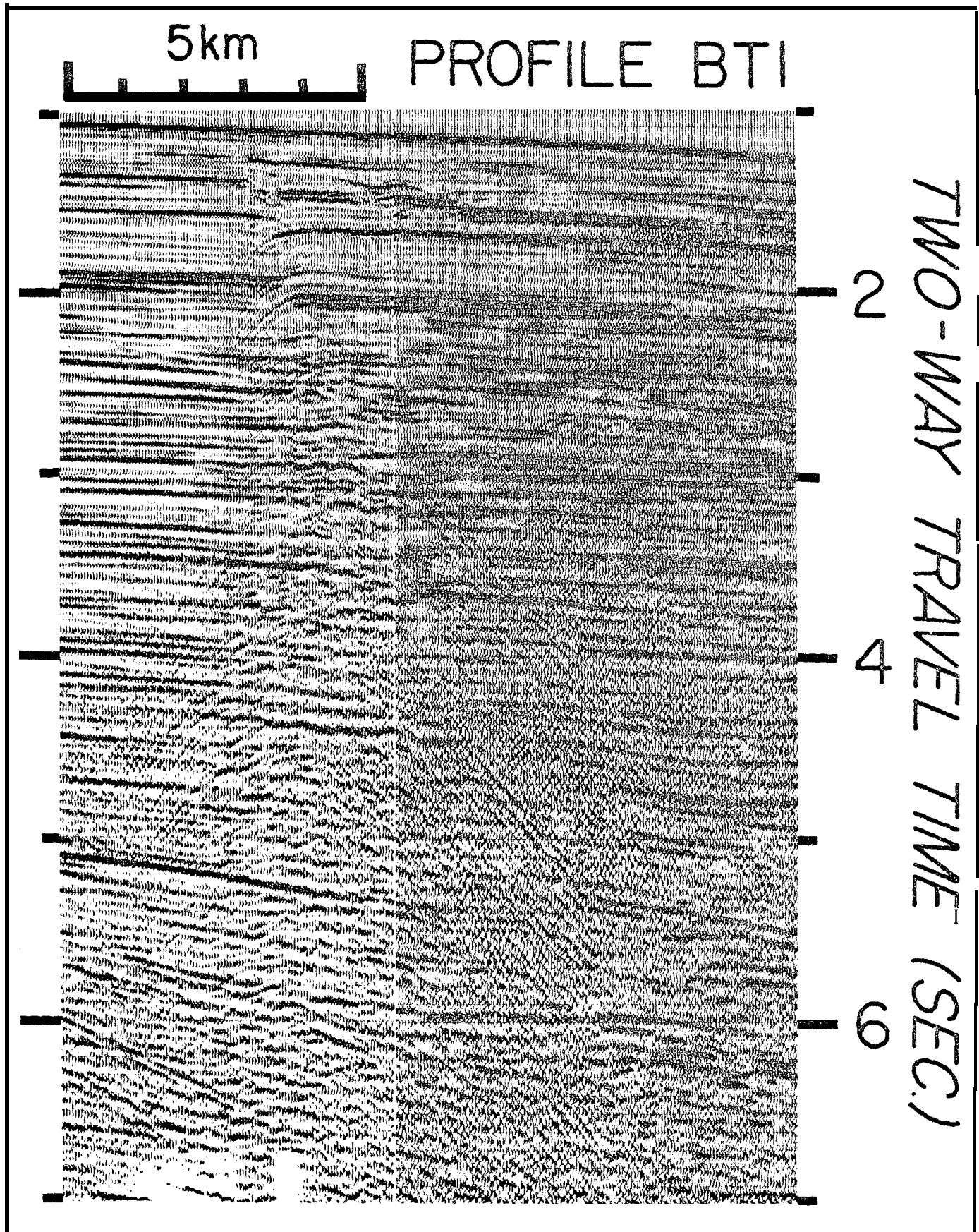


Figure 4 — Detail of seismic profile BT1, showing main growth fault. Location is shown in Figure 3.

able in many profiles. Its near-surface location is mapped in Figure 1 on the basis of both multichannel profiles and a much denser grid of single channel profiles. Hachures on the faults (Figure 1) show the downthrown side and the locations of control, where our profiles cross the fault. The main fault, shown at the left sides of Figures 2 and 3, is presented enlarged in Figure 4. We believe that certain distinctive packages of reflection events can be matched across the fault on profile BT1, allowing us to calculate throws at various depths. A plot of these data (Figure 5) shows that throw increases fairly smoothly as depth increases, indicating that the fault was active during sediment deposition (i. e., a growth fault). We believe that the fault should be termed a growth fault (Ocamb, 1961) because it shows evidence of movement during the deposition. An equivalent term is "contemporaneous fault," defined by Hardin and Hardin (1961). Our stratigraphic estimates are not sufficiently developed in this area to make a throw versus age plot. However, assuming that the long-term sedimentation rate did not vary greatly, Figure 5 suggests that movement on the growth fault at the three locations graphed was at an approximately constant average rate. Throw is observed to increase downward at

least as deep as a horizon inferred to be the top of the Jurassic (the salt is inferred to be of Early Jurassic age). Thus, the fault has been active at least since the end of the Jurassic and probably earlier. Below the inferred top of Jurassic, reflections cannot be matched across the fault.

The fault seems to continue steeply to the interpreted salt layer. On profile BT1, the fault is located well landward of the paleoshelf-slope break; it does not appear to curve and flatten into bedding, and it does not seem to have associated antithetic faults expected to exist at a fault having a curved fault plane. Thus, it is not characterized by features associated with ordinary slump-type growth faults of the continental margin. The lack of curvature on this fault is, of course, best documented on a depth converted section. One is shown in Figure 21 for a nearby crossing of the fault.

Three other faults are interpreted to exist seaward of the main growth fault (Figures 3, 6). No major movement seems to have taken place across these faults, as distinct major reflector packets are identified on both sides of the fault and show little offset.

Major erosion of outer shelf strata occurred during the cutting of the horizon A unconformity in the

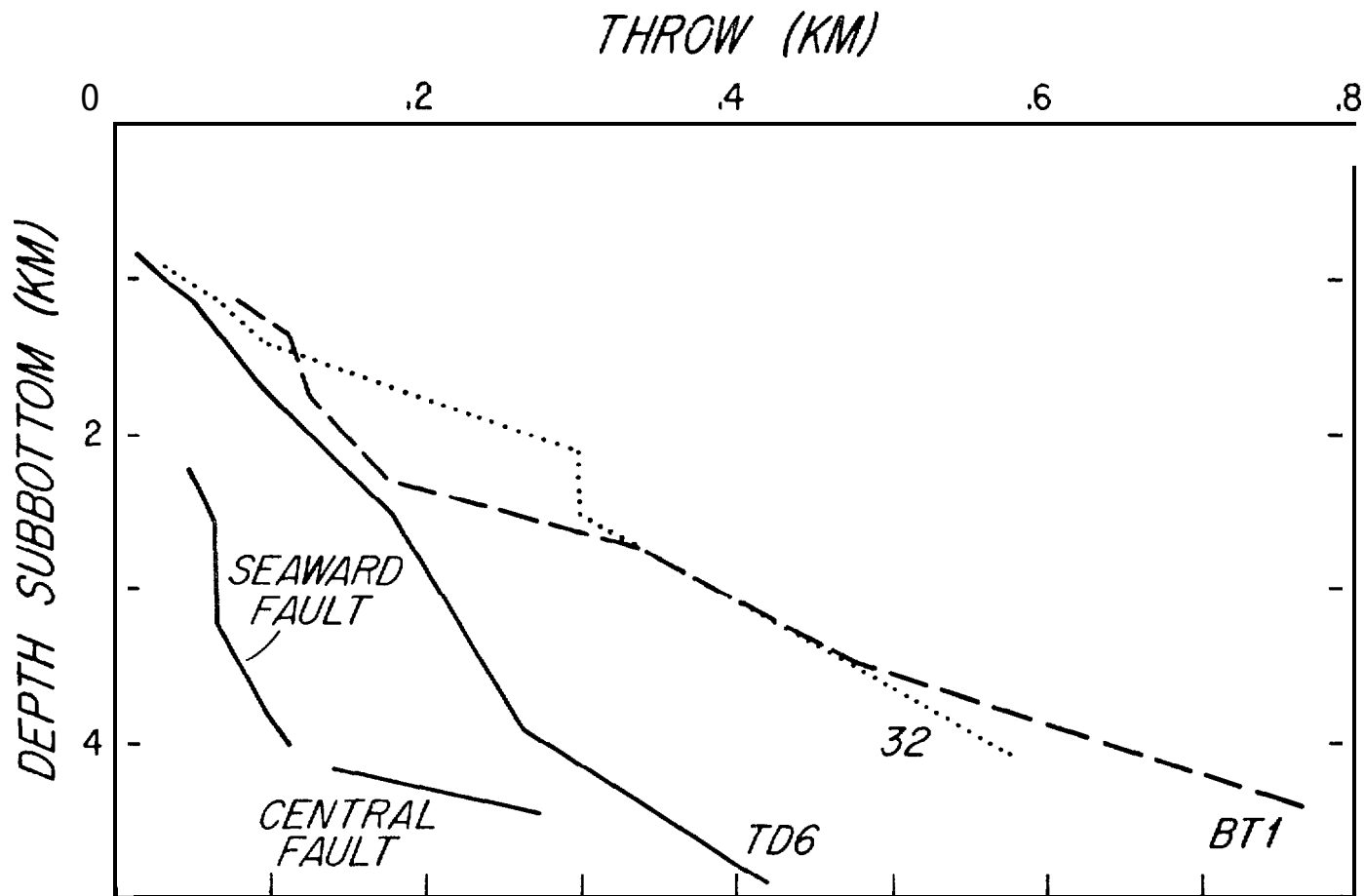


Figure 5 — Plot of throw versus depth for the faults of the three profiles discussed in the text. Solid lines identify the three fault patterns plotted for profile TD6.

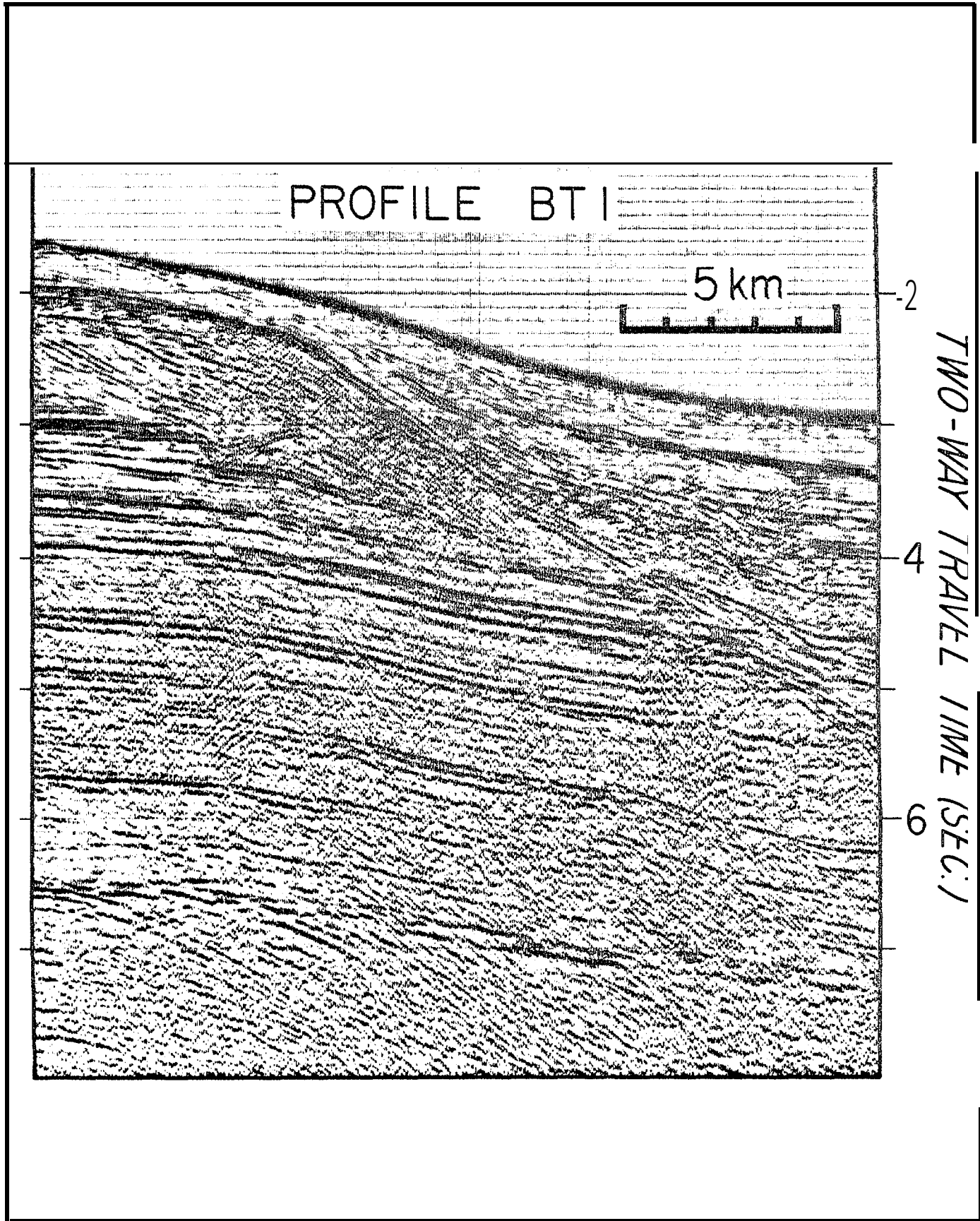


Figure 6 — Detail of seismic profile BT1 showing eroded shelf edge and several faults. Location and interpretation are shown in Figure 3.

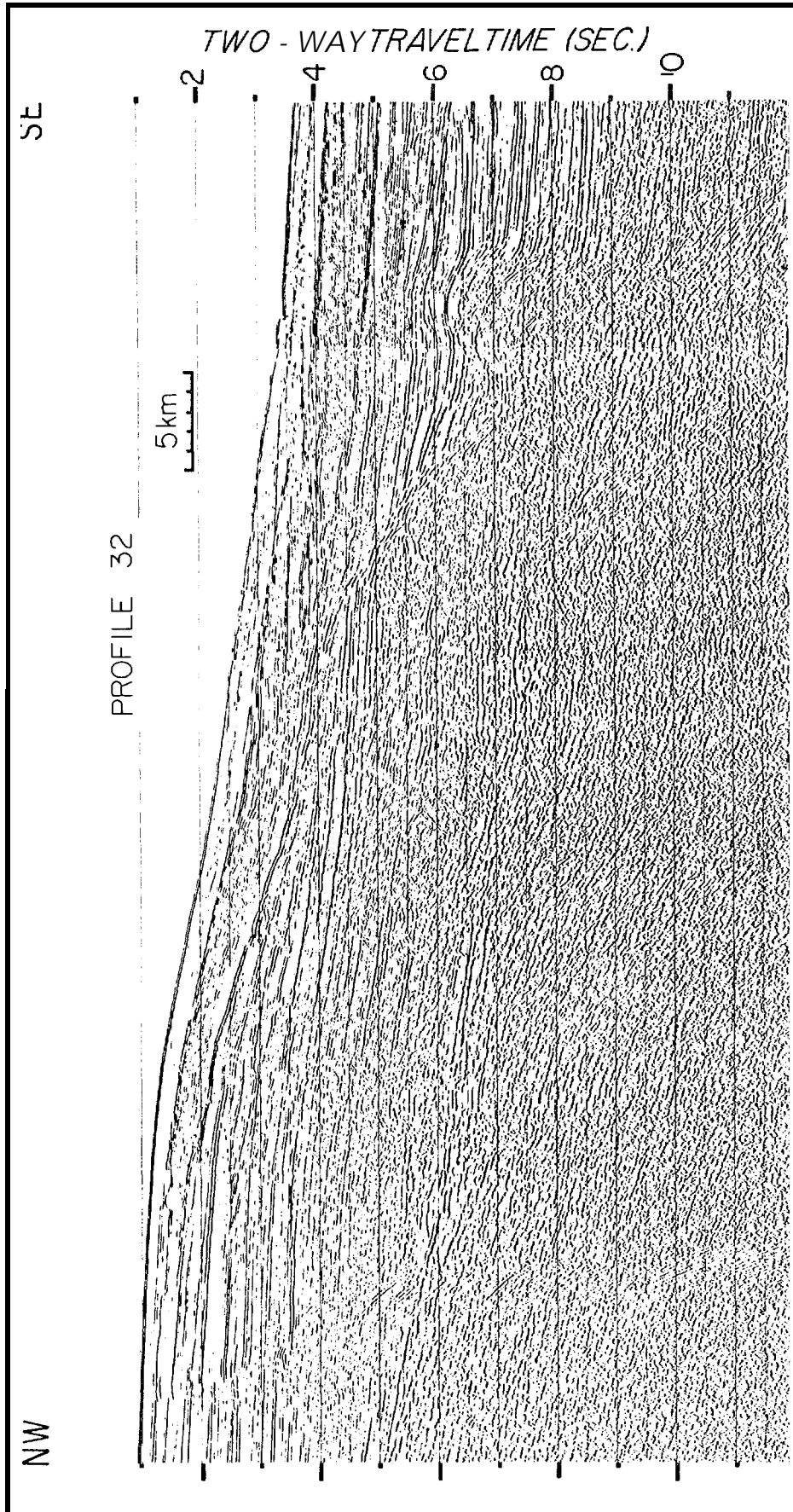


Figure 7 — Part of seismic profile 32 that crosses the Carolina Trough (northwest is to left). Profile location is shown in Figure 1. Data were collected by Geophysical Service Incorporated using a 2000-cu in (32,774 cu cum) airgun source and 48-trace, 3600-m streamer. It was processed for 48-fold stack by GSI.

western North Atlantic (Tucholke, 1979), and the results of this erosion are apparent in Figures 3 and 6. At least one previous episode of erosional retreat and progradational advance of the shelf edge also is apparent in this profile.

Seismic profile 32

Profile 32 (Figures 7, 8) also shows the major fault at the landward side of the Carolina Trough and the strong reflections inferred to come from salt. The fault (Figure 9) shows increased throw as depth increases (Figure 5) in a pattern very similar to that of the fault on profile BT1. A small diapiric upwarp is present just seaward of the eroded Jurassic and Cretaceous strata of the paleoslope (Figures 8, 10). Several subhorizontal reflection events are present beneath the paleoslope in the time section (left side of Figure 10, 4 to 8 seconds). These subhorizontal reflections, when depth corrected, show a landward dip due to the seaward-thickening water layer. This reverse dip is considered post-depositional and not associated with structure of a shelf-edge reef or bank; rather, the rotation of beds down toward the trough axis probably was caused by subsidence of the strata in the main part of the trough to the west, due to differential thermal subsidence of basement and salt withdrawal. The reduced coherence of reflection events beneath the steepest part of the eroded paleoslope probably is caused by interference of diffraction patterns generated at the rough interface of the paleoslope.

Reflections from strata just below the sea floor are partially obscured on line 32 by the blanking effect presumably produced by gas hydrates formed in the

sediments. This is particularly noticeable on the left and right sides of Figure 10. The base of the gas hydrate cemented zone forms a bottom-simulating reflector (BSR) at 0.4 to 0.5 seconds below the sea floor at the pressure-temperature limit for gas hydrate stability. A similar BSR at 0.3 to 0.5 seconds subbottom is apparent in profile BT1 (Figure 2). The BSR is very well developed in the southern part of the Carolina Trough region (Shipley et al, 1979; Dillon, Grow, and Paull, 1980; Paull and Dillon, 1981).

Seismic profile TD6

Like the other profiles shown, profile TD6 displays a main growth fault, which is part of the system mapped in Figure 1, and also some faults to the southeast that dip landward and cannot be mapped with our line spacing (Figures 11, 12; detail of profile showing faults, Figure 13). As in the previous cases shown, the landward-dipping faults are thought to terminate at depth in a salt layer, and a well-developed salt dome is present (Figure 14). The landward-dipping faults also show growth fault characteristics on this profile (Figure 5). Unlike the other profiles, TD6 displays some apparently anti-thetic faults that join the main growth fault near inflections of the fault plane (Figure 13). The deeper sections of the fault, between the inflections, become progressively steeper with increasing depth.

Downward steepening of the fault plane of the main growth fault (left fault, Figure 13) cannot be an artifact of the seismic profile because increasing velocities of deeper rocks has the effect of apparently bending *up* the fault plane in a time section, rather

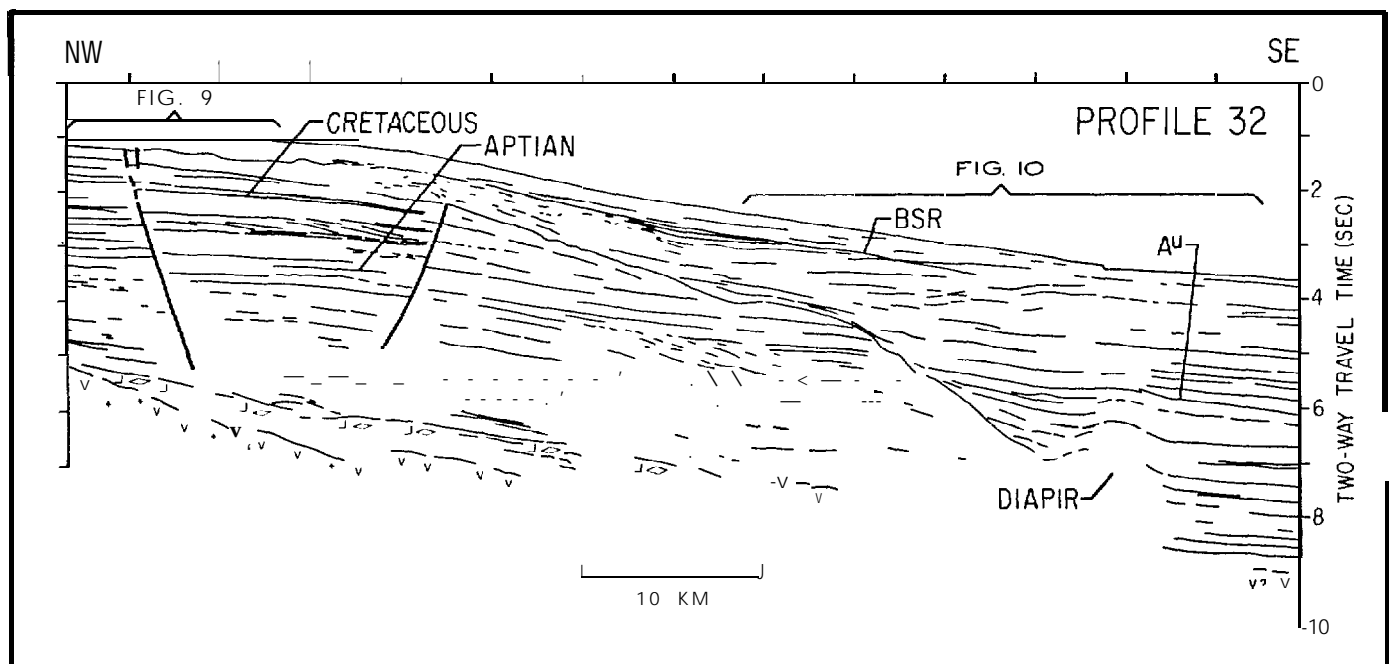


Figure 8 — Interpretation of the section of seismic profile 32 shown in Figure 7. Symbols are the same as those used in Figure 3.

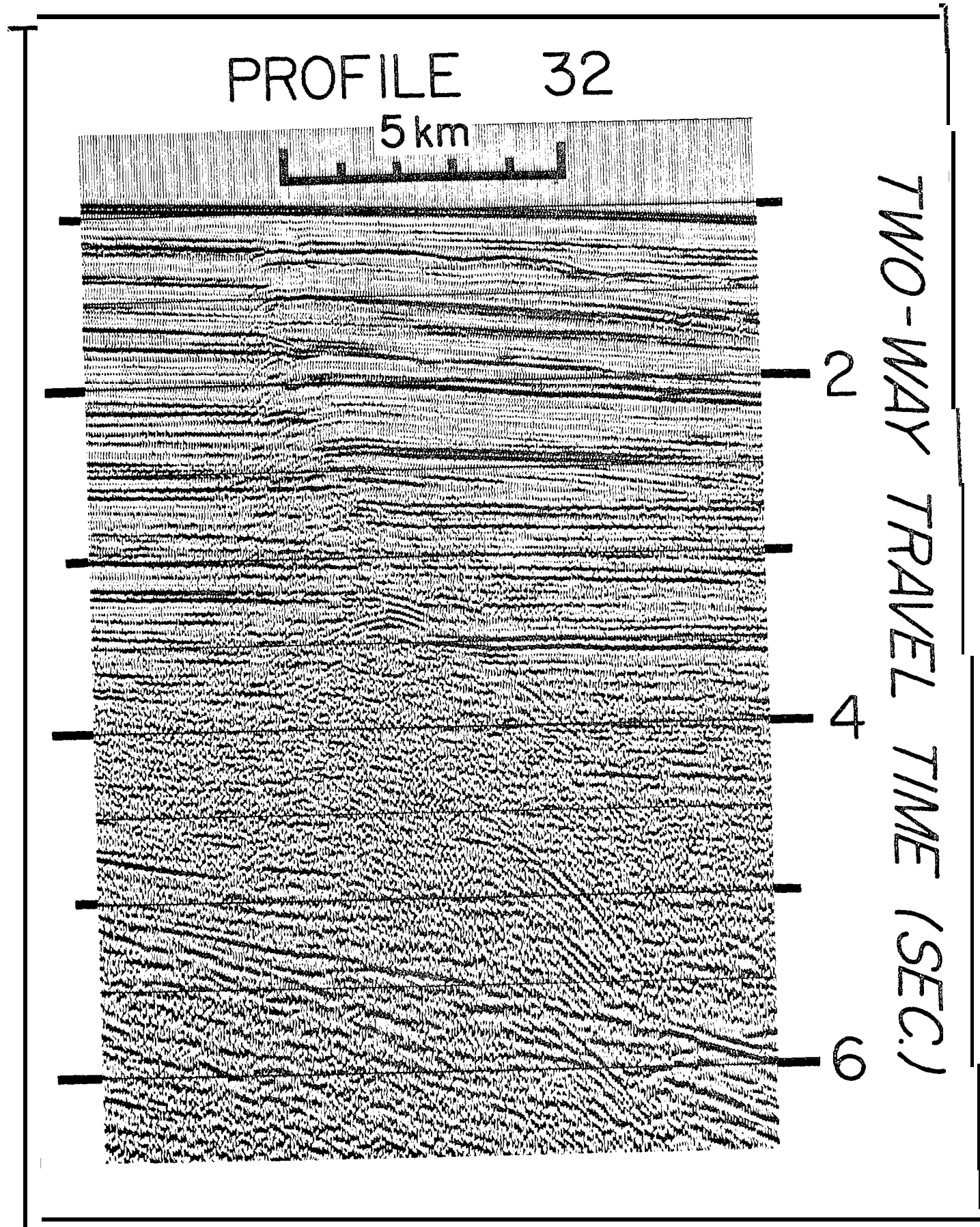


Figure 9 — Detail of seismic profile 32 showing main growth fault. Location is shown in Figure 8.

than bending it down. When these faults are replotted to true scale with no vertical exaggeration, the increasing dip with depth on the main growth fault remains. The curve of the two landward-dipping faults is nearly removed in a depth-corrected plot, indicating that those faults are almost planar.

We acknowledge that the geometry of these faults is radically different from the downward-flat tening growth faults with antithetic normal faults and roll-over structures that are ordinarily found on continental margins where high deposition rates prevail (Hardin and Hardin, 1961; Ocamb, 1961; Short and Stäuble, 1967; Lehner, 1969; Bishop, 1973; Bruce, 1973; Edwards, 1976, 1981; Weimer and Davis, 1977; Rider, 1978; Harding and Lowell, 1979). In the ordinary growth faults, not only do the faults flatten seaward, but the main faults all dip seaward except for the antithetic faults terminating in the main faults. Conversely, in the Carolina Trough we consistently observed landward-dipping faults that do not appear to terminate at depth in a seaward-dipping fault. Ordinary, concave-up growth faults show extensional

features near the fault because the seaward movement of the upper Mock by gravity gliding tends to result in opening of a gap at the shallow, more steeply dipping part of the fault. Such a gap does not actually open, of course, because it is filled by collapse of shallow strata, either by fracture (antithetic normal faults) or by plastic subsidence (rollover anticlines). Such structures are not observed in the Carolina Trough faults. Indeed, the deeper strata, in some cases (Figure 13), actually seem to have undergone shortening and been folded against the main fault. The ordinary growth fault pattern is consistent with a model in which a block slides seaward by gravity gliding (Crans and Mandl, 1981a, b), so perhaps such a model is not applicable in the Carolina Trough.

RECENCY OF MOTION OF FAULTS AND DIAPIRS

The multichannel profiles indicate that the main fault breaking the strata on the west side of the deep Carolina Trough is a growth fault, as demonstrated by the plot of throw versus depth (Figure 5). By our

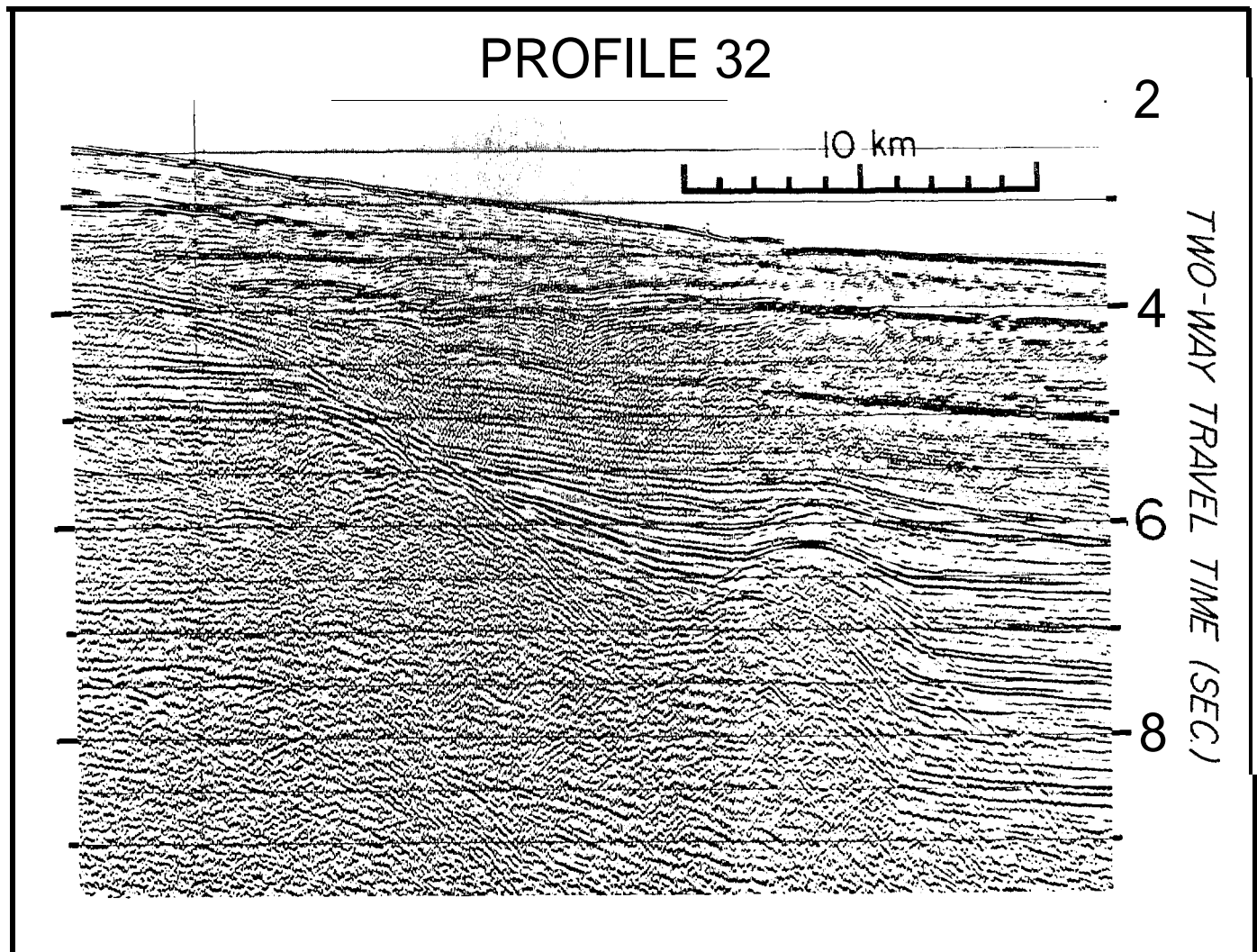


Figure 10 — Detail of seismic profile 32, showing eroded paleoslope and diapir. Location is shown in Figure 8.

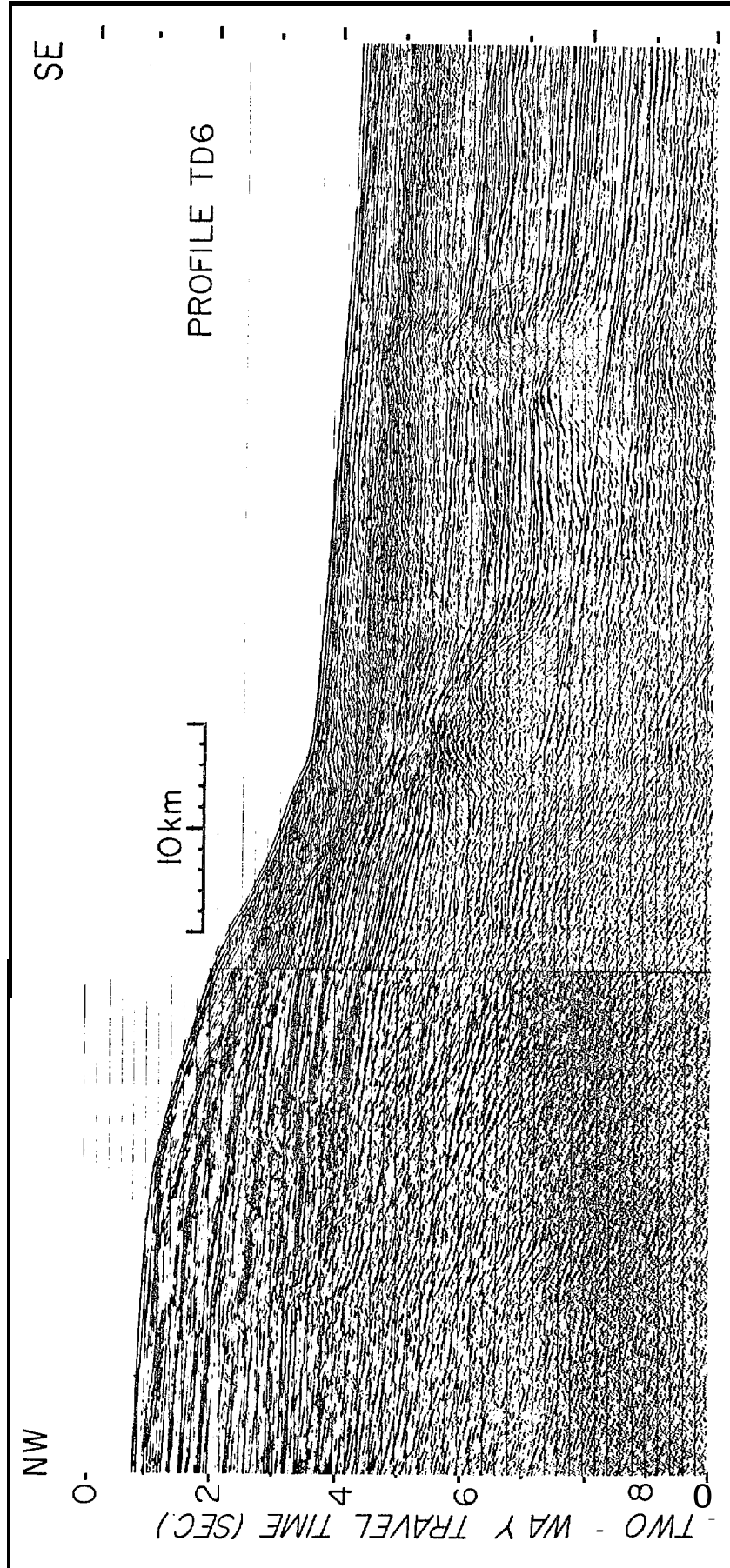


Figure 11 — Part of seismic profile TD6 that crosses the Carolina Trough (northwest is to left). Profile location is shown in Figure 1. Data were collected by Teledyne using a 2160-cu in (35,396 cu cum) array of airguns and a 48-trace, 3600-m streamer. Data were processed by the U.S. Geological Survey for a 36-fold stack.

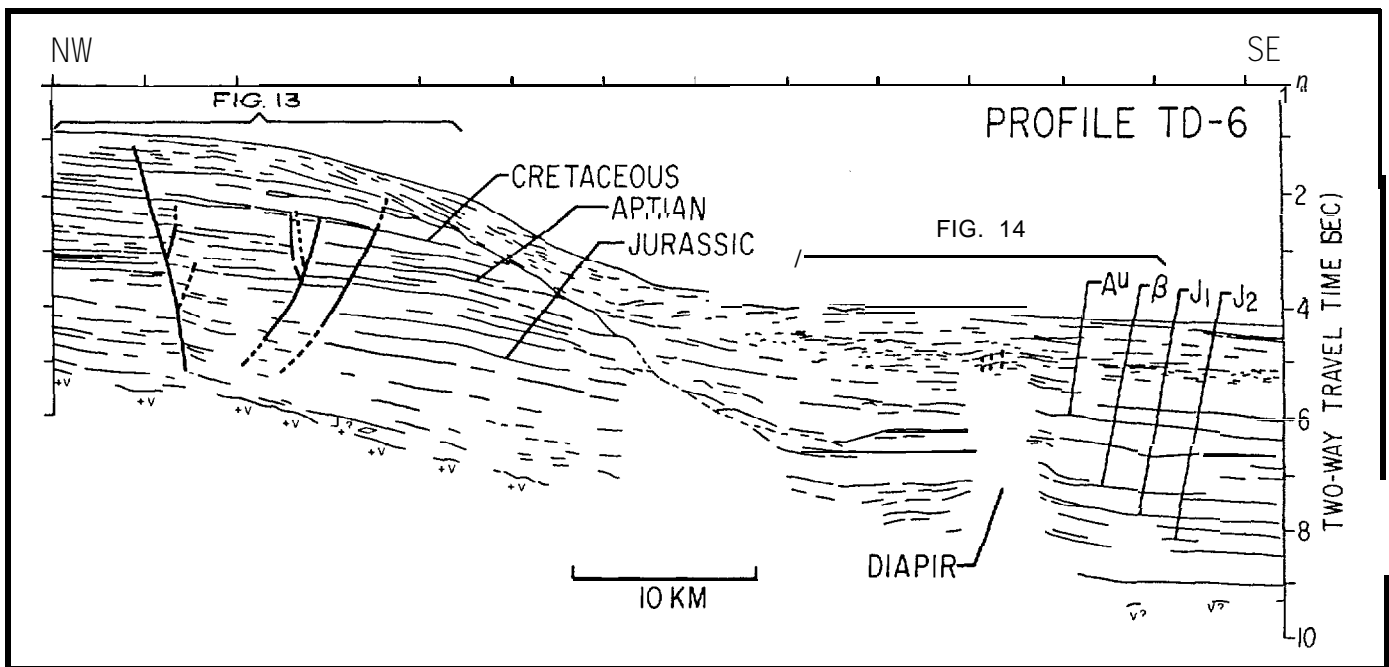


Figure 12 — Interpretation of the section of seismic profile TD6 shown in Figure 11. Symbols are the same as those used in Figure 3.

extrapolated estimates of stratigraphic horizons, we see increasing offsets back to at least the end of the Jurassic. Resolution of multichannel profiles does not allow us to define the most recent movement on the fault, so we have collected high-resolution single-channel profiles for that purpose (Sylvester, Dillon, and Grow, 1979). A high-resolution profile across the fault, 20 km northeast of profile 32 (Figure 15), shows that the effect of the fault extends to within 0.04 seconds of the sea floor (about 30 m). Breaks are not evident at that level, however, and we may be observing draping at very shallow subbottom depths. By matching packets of reflectors we conclude that a throw of about 35 m (slightly less than 0.05 seconds) exists at 200 m subbottom (0.27 seconds subbottom, or about 1.3 seconds below sea surface). Any fault showing effects so close to the sea floor in an area of deposition must be considered active.

Our detailed surveys show that diapirism is presently active because salt diapirs deform the sea floor in an area of active sedimentation. For example, Figure 16 shows a strike line through diapirs that offset the sea floor just northeast of profile 32; Figure 17 shows a dip line through the diapir that is shown in Figure 16 to have the greatest sea-floor relief. The small scarp about 13 km upslope from the diapir in Figure 17 also appears on line 32 (Figure 10). *Gloria* sidescan-sonar records demonstrate that the scarp is arcuate and about 50 km long (Figure 18). The location of this scarp and a second one to the north, as well as areas of hummocky topography adjacent to them, are mapped in Figure 1. Two high-resolution profiles across the scarp are presented in Figures 19 and 20. Strata seaward of the scarp do not appear extensively disrupted on the multichannel profile (Figure 10), but

Figures 17 and 19 show disturbance, and the sidescan record shows that the sea floor is hummocky within the arc of the scarp. Subsidence of the sea floor east of the scarp has removed support for slope sediments, resulting in a series of small slump faults (Figure 20). We conclude that the sea floor east of the scarp collapsed due to salt solution and the uplifting of the sea floor by diapiric salt flow. This collapse is continuing to create the hummocky topography.

STRUCTURAL MODEL — RELATIONSHIP BETWEEN GROWTH FAULT AND DIAPIRS

The locations of the main growth fault and the salt diapirs clearly are related to the morphology of the Carolina Trough. The growth fault is located on the landward side of the deep basin of the trough (Figure 1). The diapirs are found on the seaward side of the trough and are located on a magnetic anomaly that may arise from a basement ridge (Figure 1). The diapirs also are seaward of, and trend parallel with, the subcrop of the top of Jurassic(?) strata where it is truncated at the eroded paleoslope (line of asterisks, Figure 1). Certainly the Jurassic shelf edge was seaward of this eroded-back position, but analysis of seismic data suggests that the Jurassic shelf edge was not far seaward of the position and, therefore, the diapirs probably rose beneath the Jurassic continental slope.

We suggest that salt was deposited in the deepest part of the Carolina Trough, and that it was loaded by sediments during the Jurassic and began to flow seaward and migrate into rising domes (Parker and McDowell, 1955; Humphris, 1979). The location of the domes probably was controlled by a shallowing of

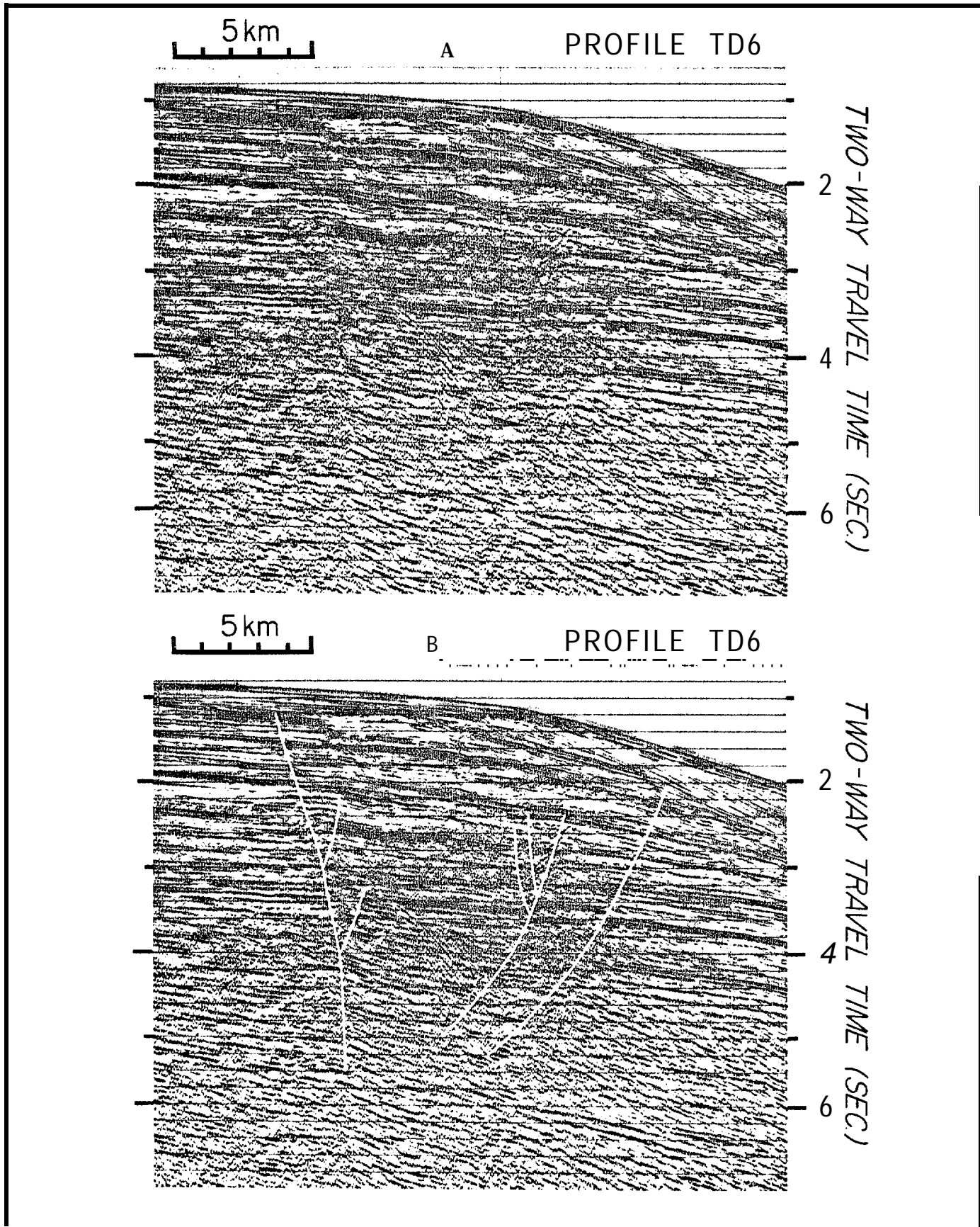


Figure 13 — Detail of seismic profile TD6 showing faults. Location is shown in Figure 12. Part A shows unmarked record; part B shows interpreted faults.

basement at the seaward side of the trough, which caused the salt to begin to flow upward and by the position of the shelf edge, seaward of which overburden pressure on the salt was reduced. Removal of a volume of salt resulted in subsidence of the block of sedimentary rock above the area of the original salt-depositing pan. At the landward side of the pan, subsidence of that block caused a fracture in the sedimentary strata and, because the flow of salt continued for a long period (and still continues), the fault was active throughout this period. Thus, the growth fault formed because of continual removal of support from a major block of the continental margin strata by salt flow, and the location of the fault marks the

landward limit of significant salt deposition. This volume-transfer model is indicated graphically on a depth-converted seismic profile in Figure 21. Narrow, half-barbed arrows indicate subsidence along the fault and broad arrows show proposed salt flow.

Such a volume-transfer model requires that the volume lost in subsidence of the block of strata in the Carolina Trough must be equal to the volume of salt removed, which is represented mainly by the volume in the domes. Neither of these volumes can be calculated accurately, but by measuring the area of the subsiding block and estimating an average throw that we infer from profiles, and by measuring the area of observed domes and estimating an average height, we

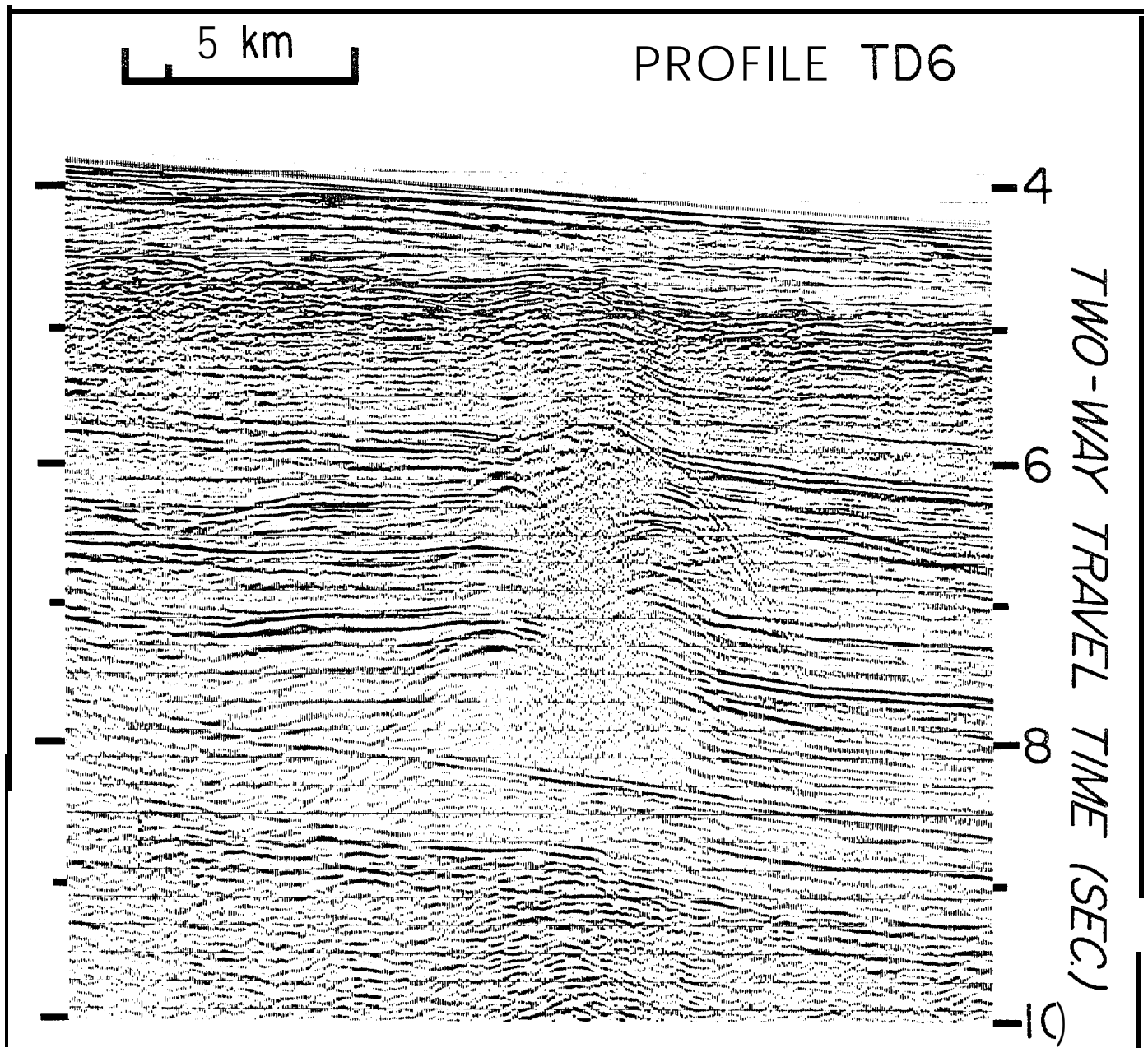


Figure 14 — Detail of seismic profile TD6 showing diapir. Location is shown in Figure 12. Reflections that apparently pass through the diapir at about 8.2 seconds depth and deeper are multiple reflections.

can make approximations of salt volume lost and gained. Both will be minimum values. The subsidence calculation will be a minimum because our estimated throw is measured no deeper than the top of the Jurassic owing to the difficulty in matching reflector packages at greater depth in the seismic record, and so throw probably is greater than we determined. Salt-dome volume represents a minimum because we must have missed some domes. Calculated values are 4,400 cu km lost in subsidence and 4,100 cu km of salt added to the slope in the salt domes. The agreement probably is fortuitous, but the general correspondence is encouraging for our structural model.

Faulting due to salt withdrawal has been identified

by various authors (Lehner, 1969; Seglund, 1974; Hospers and Holtke, 1980), but generally it is associated with an extensive layer of salt. In the Carolina Trough a narrow, linear salt-depositing basin resulted in formation of a linear fault when salt flow and subsidence occurred. Seglund (1974) defined faults due to salt withdrawal as "collapse faults," but since this term requires the inference of salt flow, rather than being simply descriptive of fault geometry, we prefer the term growth fault. Apparently the block of strata within the Carolina Trough subsided nearly vertically. A more common situation seems to entail generation of a series of seaward-dipping growth faults by seaward-directed gravity gliding of blocks of strata,

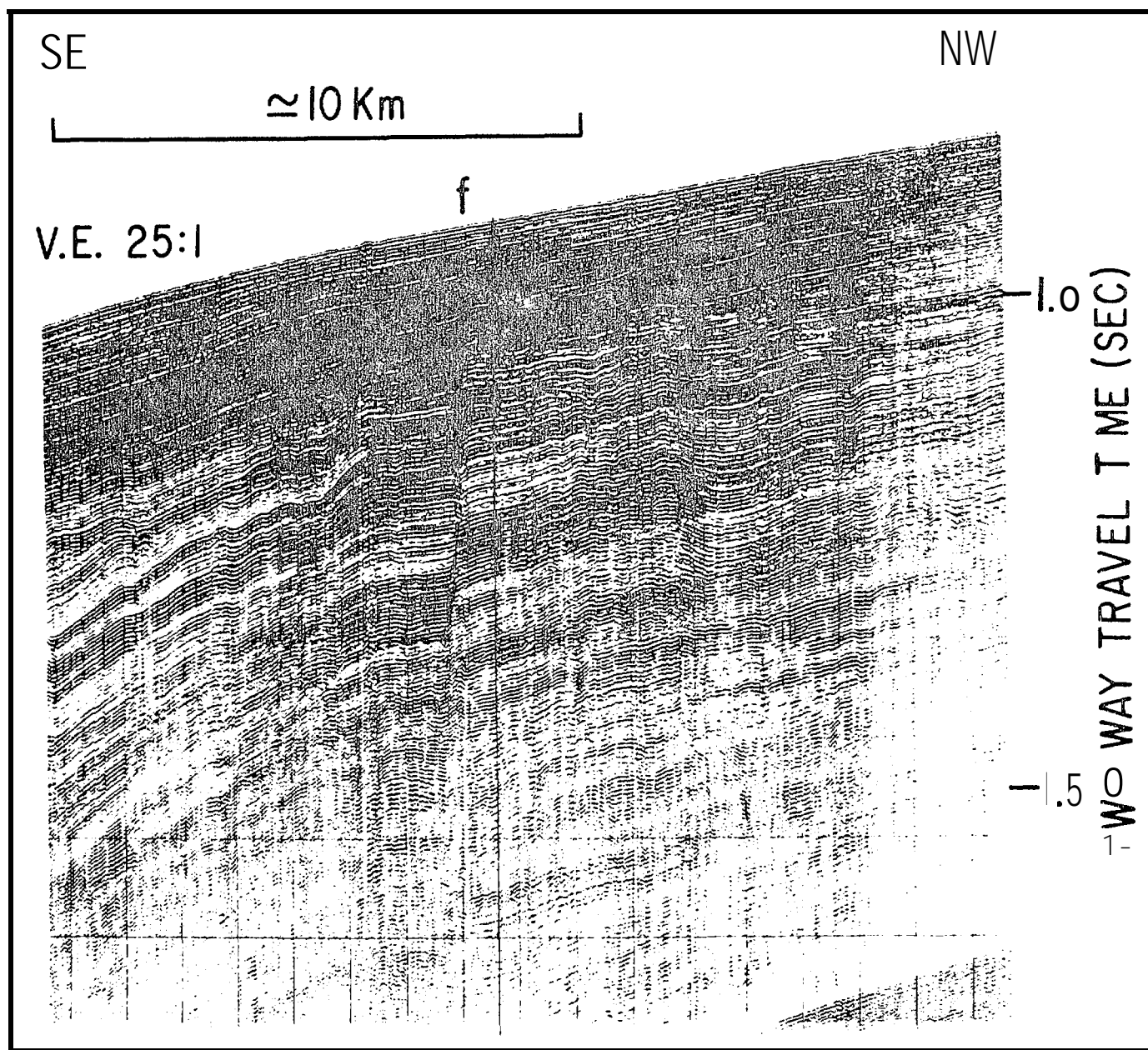


Figure 15 — Single-channel, high-resolution airgun profile across the growth fault. Fault is marked by f. Profile is located 20 km northeast of profile 32.

perhaps on a lubricating layer of salt or shale (Cloos, 1968; Bishop, 1973; Bruce, 1973; Edwards, 1976; Weimer and Davis, 1977; McPherson, 1978). Such seaward movement commonly generates extensional structures (rollover anticlines and antithetic normal faults) at the steeper shallow part of the concave-up fault (Short and Stäuble, 1967; Bruce 1973; Edwards, 1976, 1981; McPherson, 1978; Harding and Lowell, 1979). As noted in the discussion of profile TD6 (Figures 12, 13), we have a totally different structural style

in the faults of the Carolina Trough. The main seaward-dipping growth fault is essentially planar, as shown in the depth converted profile of Figure 21, or, in one crossing, even concave-down (Figures 12, 13); faults at the outer part of the Carolina Trough dip landward rather than seaward, and we have some evidence of shortening of strata by folding against the growth fault in the deeper part of the trough (Figure 13).

Why does the faulting of the Carolina Trough take

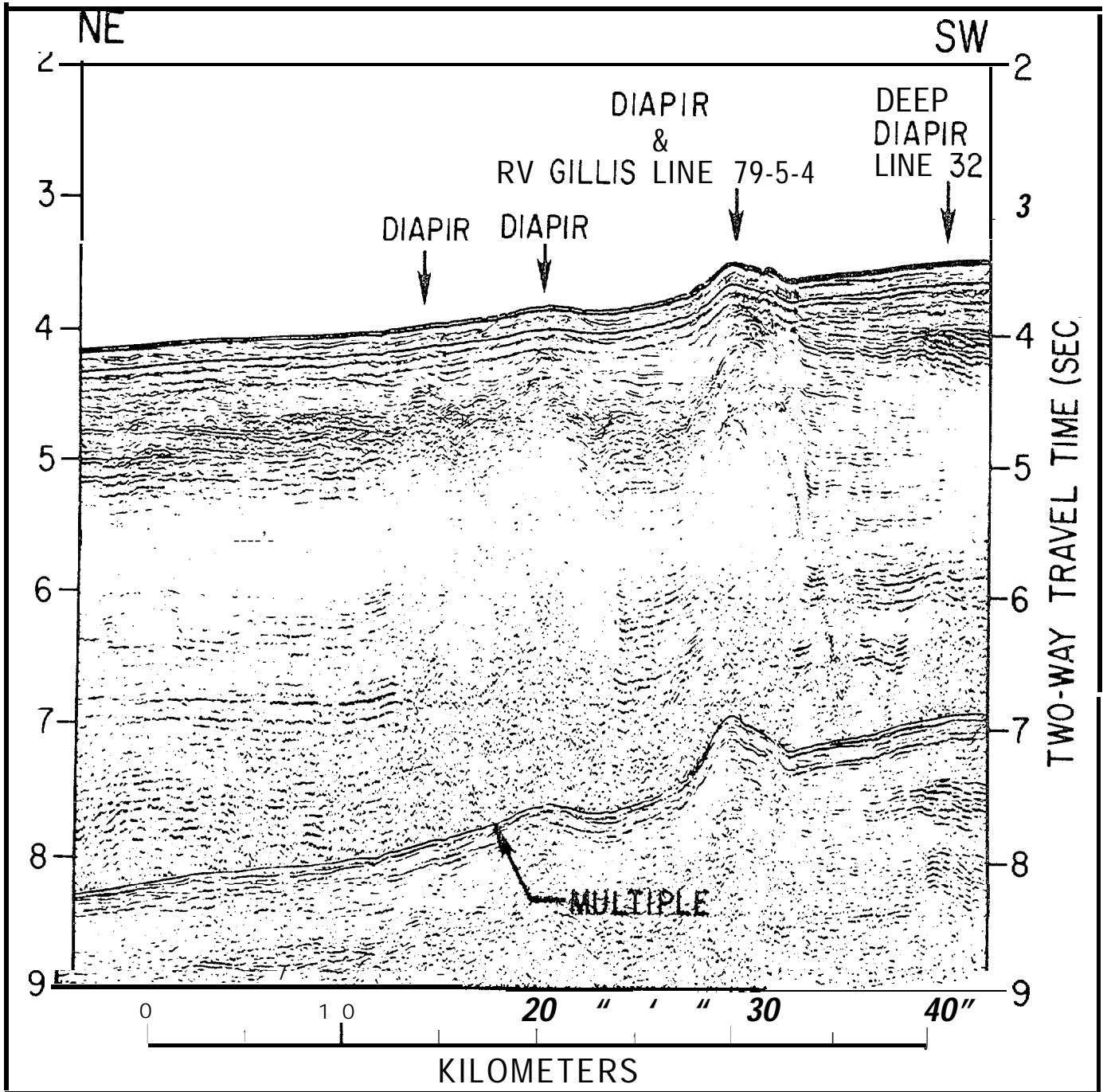


Figure 16 — Single-channel airgun profile along diapir trend near profile 32,

this unusual pattern? One reason may be the presumed narrow zone of salt deposition (perhaps 30 to 40 km wide) which did not provide an extensive lubricating layer on which the old slope and rise deposits could slide seaward; thus they acted as a buttress. The basement ridge inferred from magnetics at the seaward side of the trough may have added to this buttressing effect. Furthermore, the rising salt domes themselves may have created a discontinuous uplifted ridge at the seaward side of the trough. This ridge

could have inhibited seaward gliding of the sediment block within the trough by creating a tendency for sediment to slide landward into the trough. The landward-dipping faults may result partly from relative subsidence off that ridge, in a manner similar to that suggested by Quarles (1953) or Bruce (1973).

You would expect vertical subsidence of the block of sediment between two troughward-dipping fault sets to produce some compression, and we have evidence of that in the folding against the fault plane. You

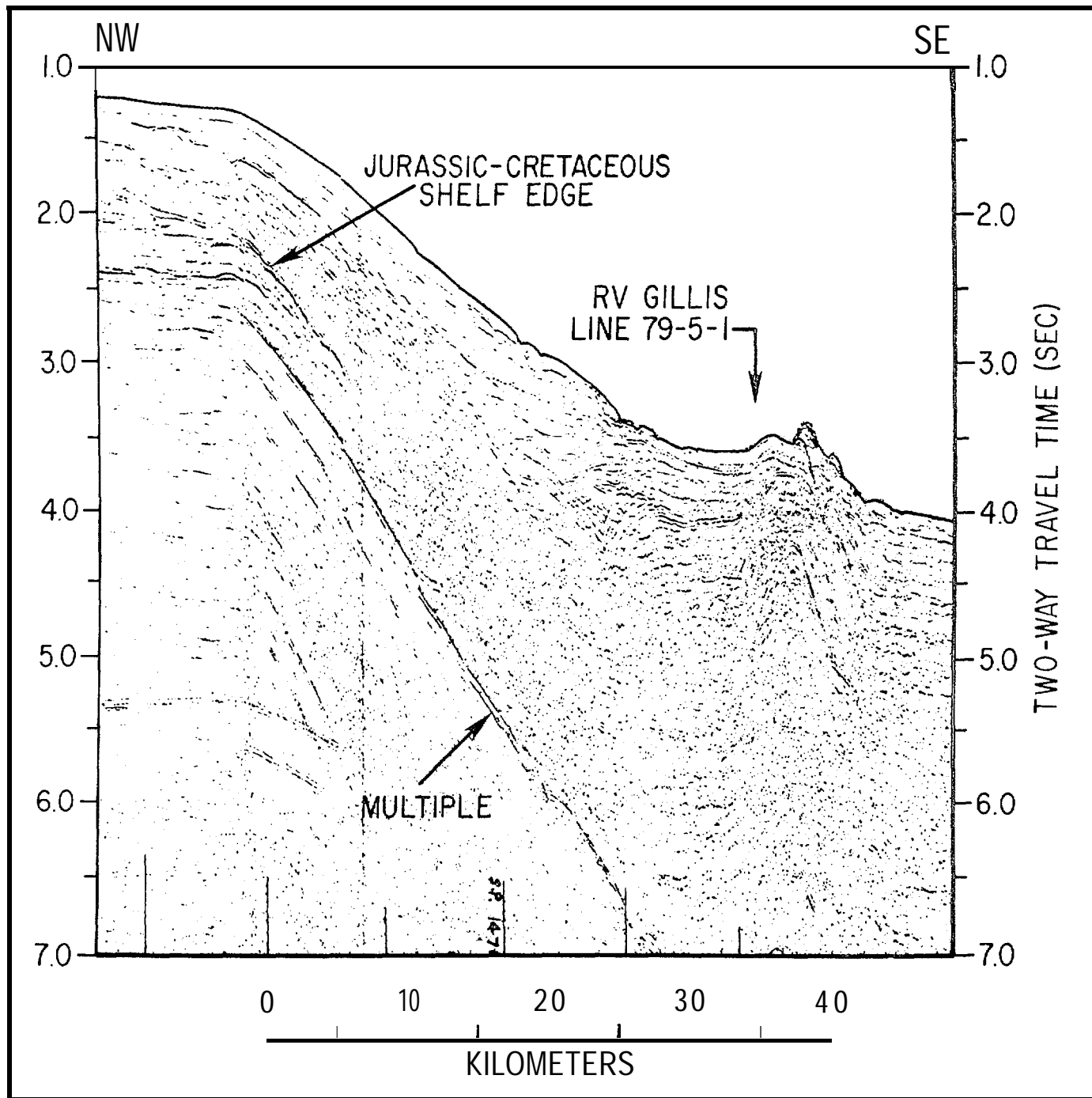


Figure 17 — Single-channel airgun profile across diapir that has disrupted sea floor. The scarp is less obvious here than in Figures 19 and 20; it occurs 13 km northwest (left) of the highest peak of the diapir.

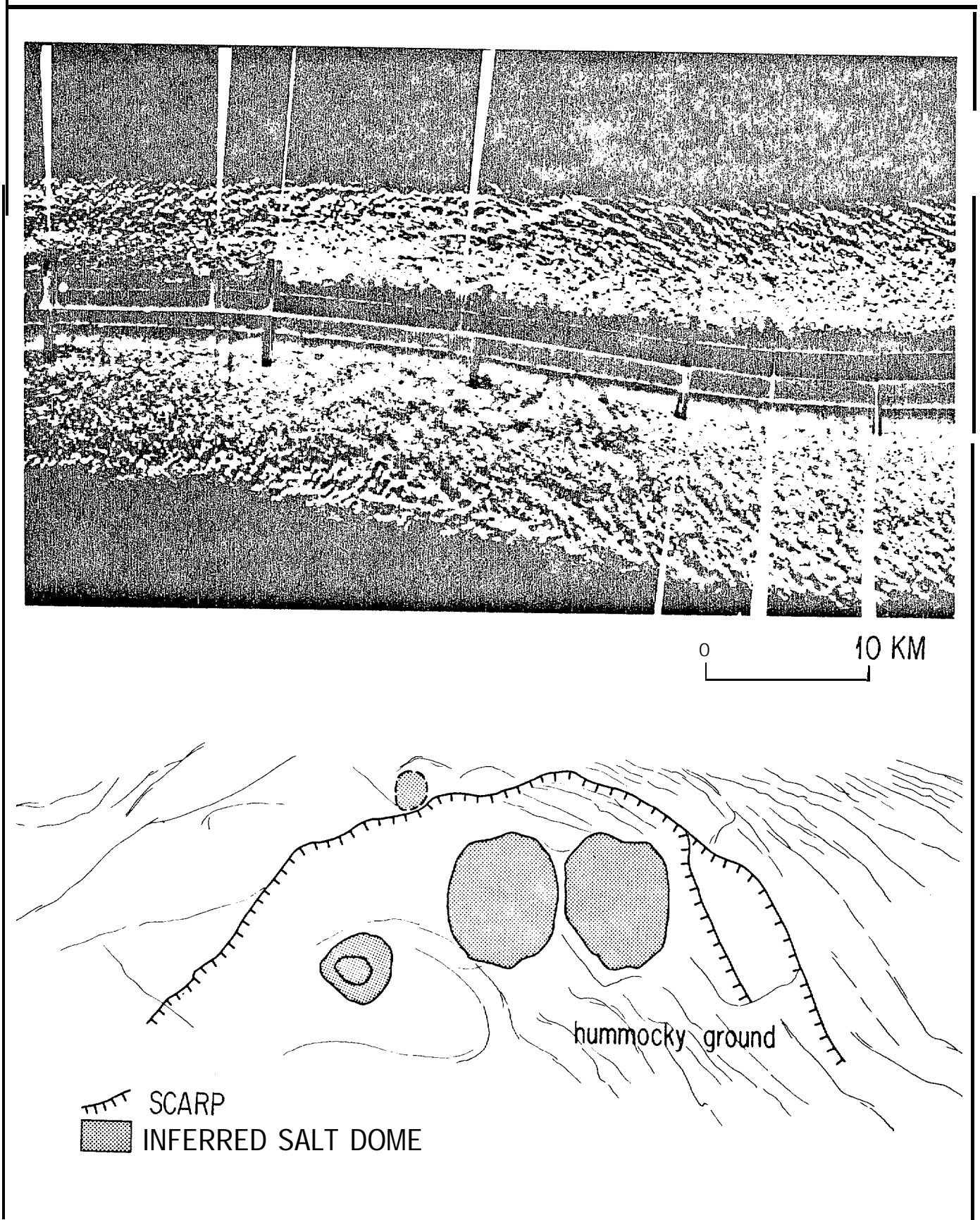


Figure 18 — Long-range (*Gloria*) sidescan-sonar record of part of the diapir trend with interpretation. This shows the southern of the two areas of hummocky sea floor, bounded by scarps to the northwest, that are indicated in Figure 1.

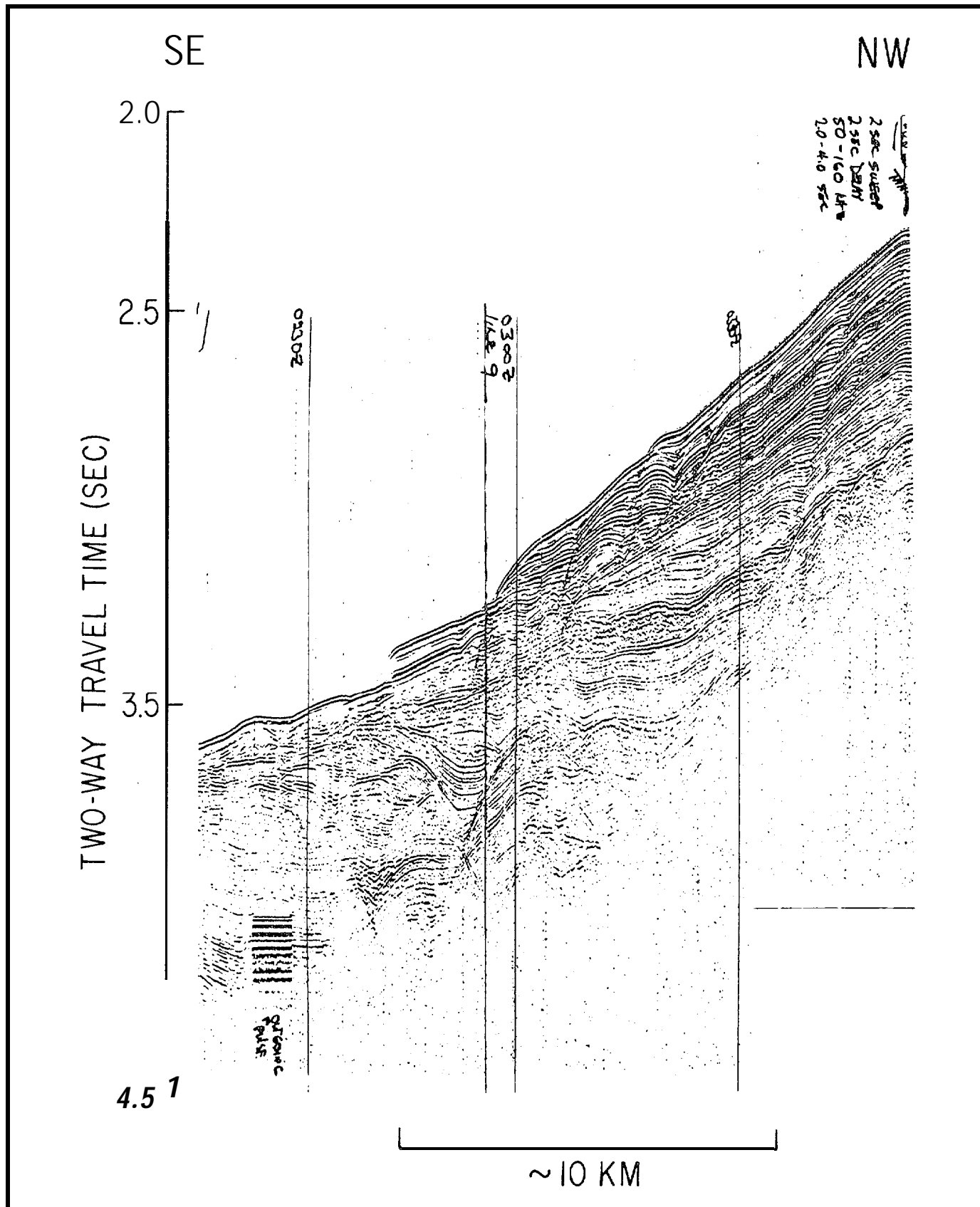


Figure 19 — Single-channel, high-resolution airgun profile across the southern part of the scarp that is shown in the *Gloria* sidescan sonar-record of Figure 18. Note disturbed strata and irregular sea floor downslope from the scarp. Vertical exaggeration is 14:1.

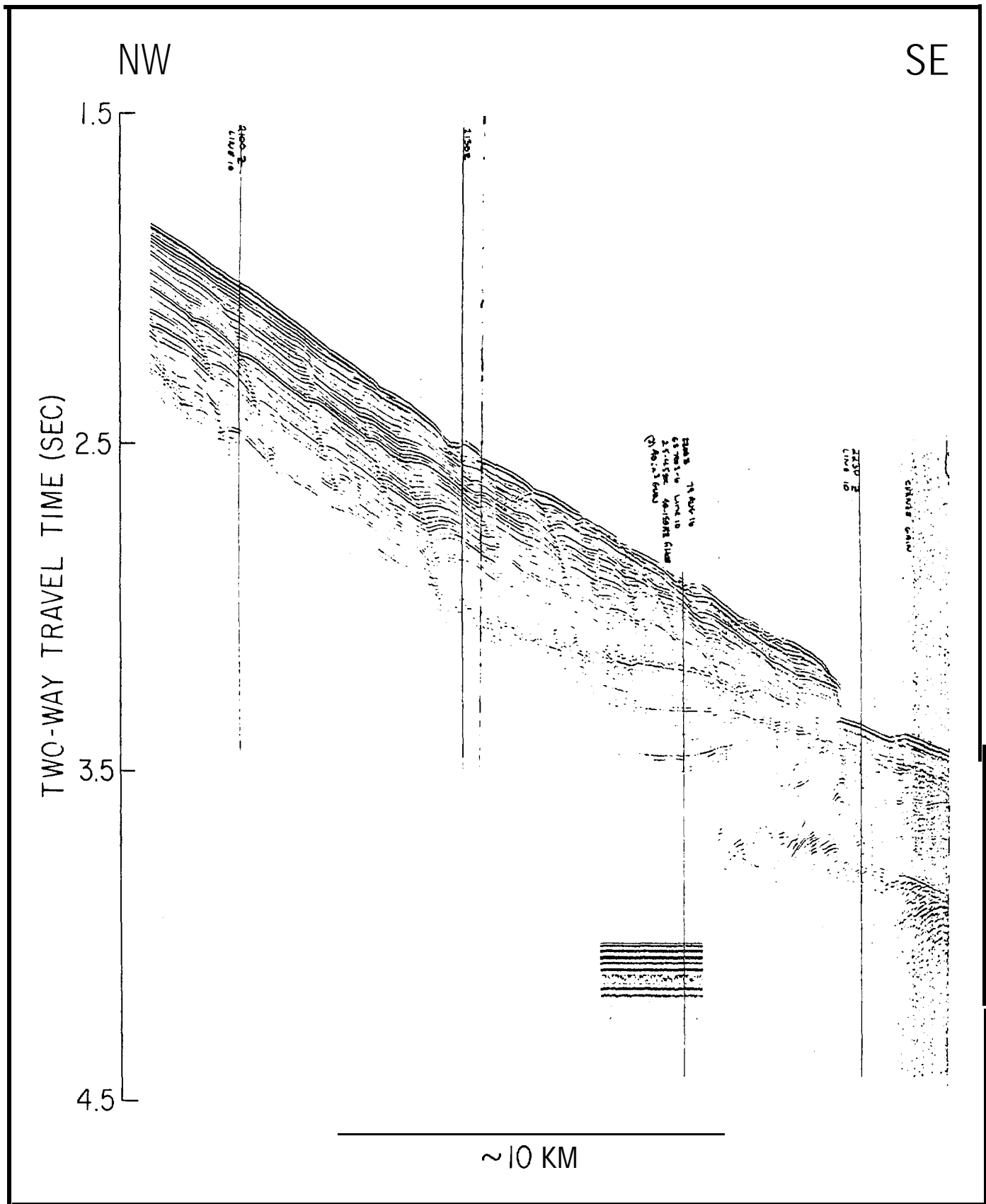


Figure 20 — Single-channel, high-resolution airgun profile across the southern part of the scarp that is shown in the *Gloria* sidescan-sonar record of Figure 18. Note fairly evenly spaced small slump faults, apparently resulting from removal of support at the scarp. Vertical exaggeration is 11:1.

should also expect downfaulting, with a downward steepening fault plane (concave down), to produce compression against the fault that would be greater on the shallower part of the fault plane than at depth. That is, there would be a tendency to lift up the shallower part of the subsiding seaward block, the part above the flatter, shallower part of the fault. Such a situation is interpreted at the main growth fault (left fault) in Figures 12 and 13. We propose that the apparently antithetic faults that join the main growth fault at its inflections (left fault, Figure 13) are agents to release such compression. Because the strata to the right of the apparently antithetic faults are subsiding and the faults dip to the left, they are by definition reverse faults. In such a case, where downfaulting occurs at a steep angle against a normal fault that steepens with increasing depth, compression is generated against the fault plane. That compression, which is greater at the shallow part of the fault, can be released along reverse faults that terminate in the main normal fault. We informally have termed such reverse faults "wedge faults."

REGIONAL CONTROLS ON SALT DEPOSITION AND DIAPIR FORMATION

Diapirs are common on the seaward sides of the Carolina Trough (Figure 1) and also the Scotian Basin (Jansa and Wade, 1975), yet, although profiling cover-

age is intensive, they appear to be relatively scarce elsewhere on the eastern North American continental margin (Figure 22). Diapirs are present to a very minor extent east of Florida in the Bahamas (Ball, Gaudet, and Leist, 1968), in the Baltimore Canyon Trough (Grow, 1980), and on eastern Georges Bank. The domes on eastern Georges Bank are an extension of the Scotian Basin diapirs (Uchupi and Austin, 1979). Salt has been drilled in the Bahamas (Tator and Hatfield, 1975), Baltimore Canyon Trough (Grow, 1980), and Georges Bank (Amato and Simonis, 1980). Consequently, we conclude that salt deposition probably was nearly universal during early stages of continental margin formation off eastern North America (also suggested by Evans, 1978), but that domes formed extensively only in two areas, the Scotian Basin and the Carolina Trough. We question the armor-plate theory — that thick salt may exist, yet not flow into domes because of a strong, rigid, rock layer above it. Some zones of relative weakness should be expected, allowing passage of salt. We prefer the argument that presence of diapirs simply indicates the former presence of a thick layer of salt. Therefore, we suggest that a thickness of salt sufficient to allow generation of extensive groups of domes accumulated only in two regions.

Why are thick deposits of salt concentrated only in these two basins? Some earlier conclusions (Burke, 1975) based on less data do not seem to apply. Thick

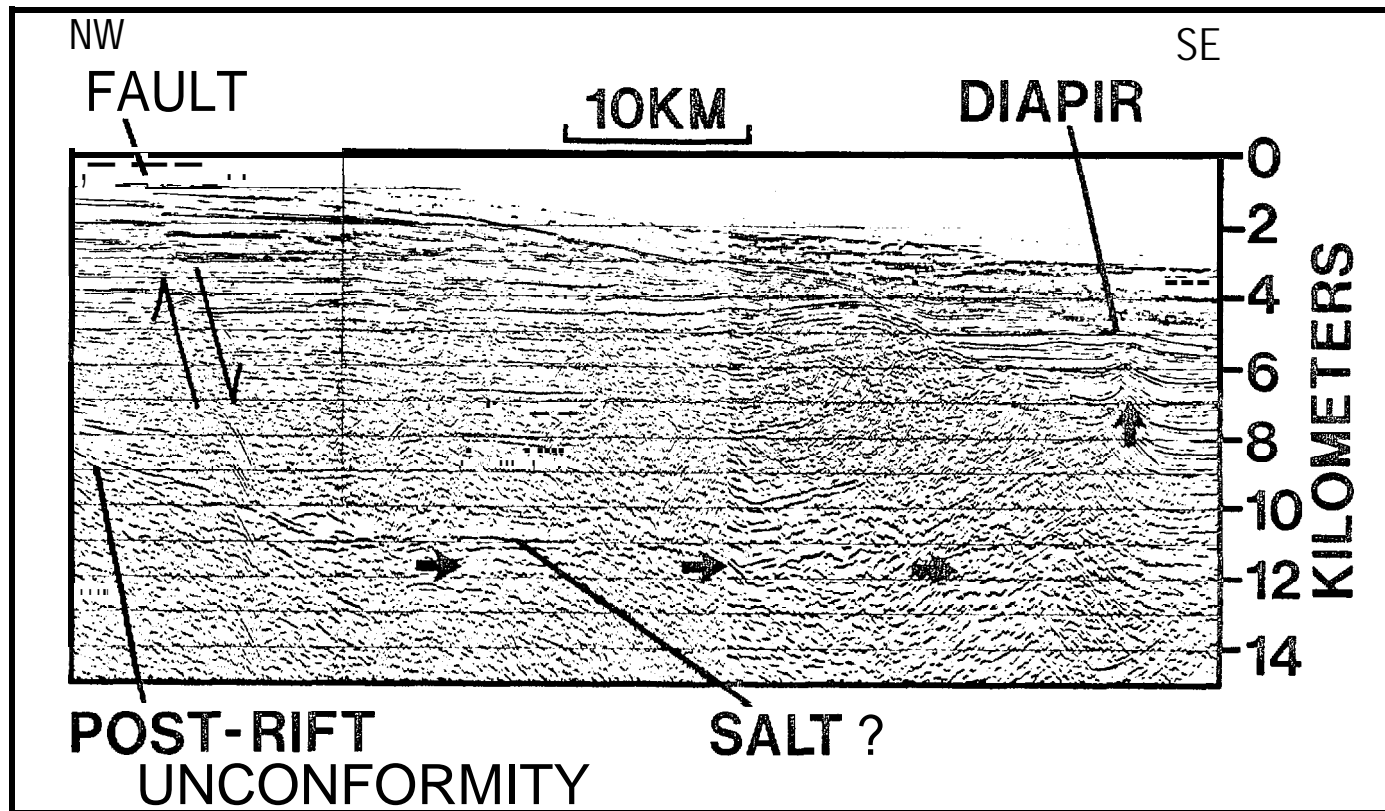


Figure 21 — Depth-converted part of seismic profile 32 across the Carolina Trough. Compare this to Figure 7 that shows the same profile in a time section. Single-barbed arrows show relative motion on the growth fault that we believe has resulted from salt flow into diapirs. Direction of inferred salt flow is shown by broad arrows. Vertical exaggeration is only 2:1.

salt deposits are not restricted to the vicinity of an ocean spillway (Figure 22); they do not seem to be restricted by obvious high tectonic barriers or former hot-spot locations and they probably are not controlled by latitudinal climatic zones. Indeed, a continent as large as Pangea probably always had a dry zone near its center, which would mean that the entire newly-formed Atlantic margin was located in a dry area.

We propose that thickness of salt in continental margin basins and, ultimately, the presence or absence of extensive salt domes were controlled by timing of

early basin subsidence. The timing was determined by the amount of stretching and thinning of basement during the rifting stage. Basins having greater thinning of basement would have subsided below sea level sooner and, therefore, received oceanic waters for a longer time before the opening ocean developed a circulation connected to the world ocean that terminated salt deposition. Because they underwent a longer period of salt deposition, these early-subsiding basins probably accumulated a thicker salt layer. The few available crustal sections across the margin, based on gravity and refraction, support this conclusion by

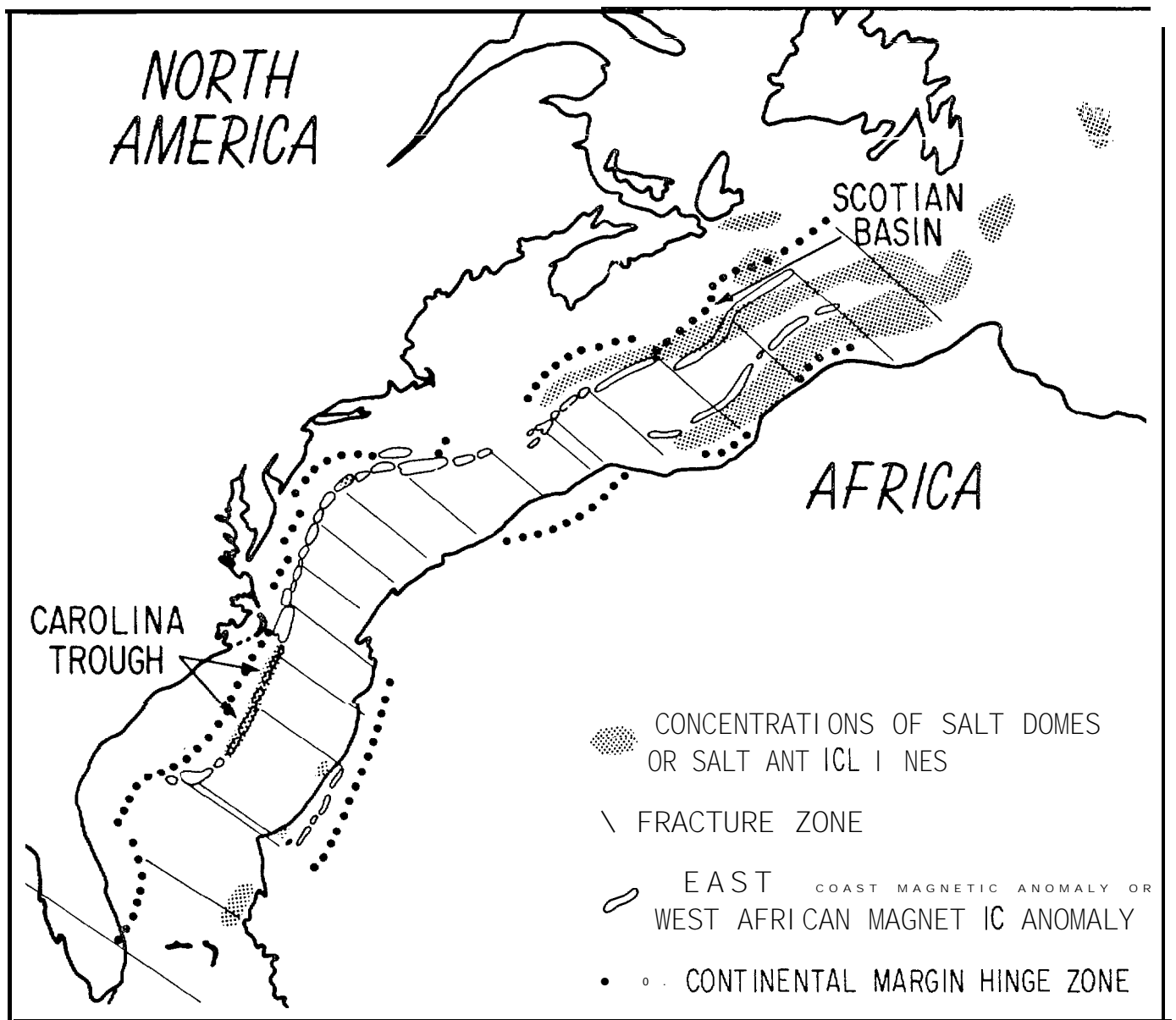


Figure 22 — Reconstructed locations of major continental blocks during early ocean opening in Middle Jurassic time. Locations are shown for known diapirs or diapir groups that presumably were forming by this time (Aymé 1965; Ball, Gaudet, and Leist, 1968; Templeton, 1970; Grunau et al, 1975; Jansa and Wade, 1975; Hinz, 1977; Uchupi and Austin, 1979; Grow, 1980; Jansa, Bujak, and Williams, 1980).

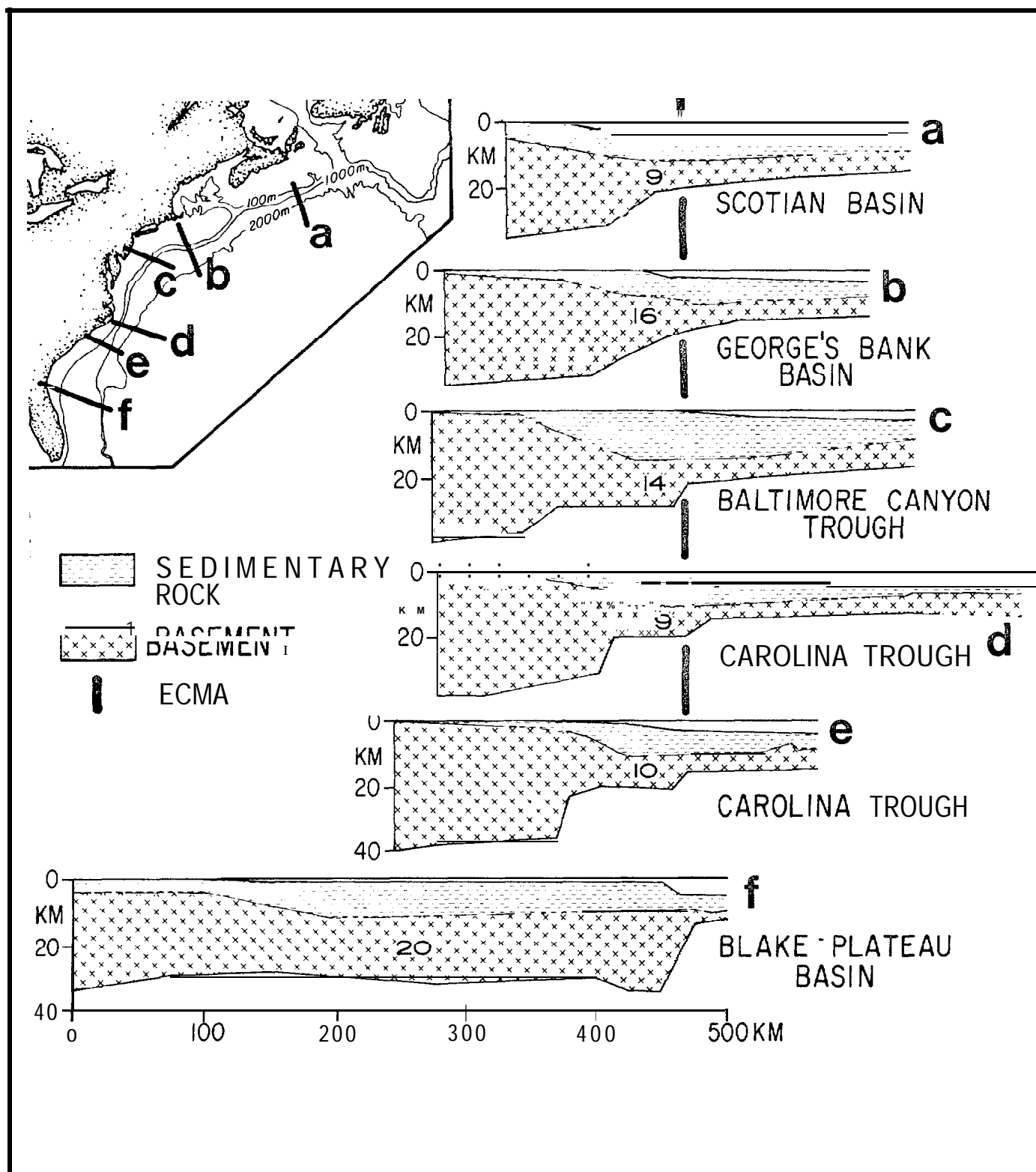


Figure 23 — Simplified crustal sections across the basins of eastern North America based on gravity and refraction (Keen et al 1975; Grow, Mattick and Schlee, 1979; Kent, Grow and Dillon, 1979; Grow, 1980; Hutchinson and others, this volume). Numbers in section indicate basement thickness at the locations of the numbers, which are placed approximately at the centers of basins. More recent interpretation of the Scotian Basin data suggest that the basin basement may be somewhat thicker than indicated, perhaps 11 km, (C. E. Keen, C. Beaumont and R. Boutilier, this volume). The profiles are aligned along the East Coast Magnetic anomaly (ECMA) except for the Blake Plateau Basin profile, where the ECMA is not present. Section "b" actually is to the west of the main part of the Georges Bank Basin and crosses a sub-basin of the Georges Bank system; it is well away from the diapirs that extend down from the Scotian Basin.

showing that basins associated with many diapirs (Carolina Trough and Scotian Basin) have basement thicknesses at the basin axis of 9 to 10, perhaps 11, km (Figure 23). Conversely, other basins, those without abundant diapirs, show basement thicknesses of 14 to 20 km.

SUMMARY

1. The Carolina Trough is a long (450 km), narrow (40 km), linear basin off eastern North America.

2. A group of salt diapirs is aligned along the seaward side of the trough. The diapirs are located at a magnetic anomaly on the seaward side of the basin that may mark a basement ridge or step that could have controlled upward flow of salt.

3. A normal fault follows the landward side of the Carolina Trough. It is a growth fault, as is shown by a pattern of throws increasing as depths increase. Unlike ordinary continental margin slump-type faults, the growth fault does not flatten into bedding nor does it have antithetic normal faults. The fault generally continues steeply down to a strong reflector that may represent the salt horizon in the trough. At one location, the fault steepens at depth and may have reverse faults associated with it that were created by this steepening of the fault plane.

4. The growth fault probably resulted from removal of support as salt flowed seaward into the domes from the deep part of the trough. This transfer of volume from the deep trough resulted in slow subsidence of a large block of strata as the domes rose.

5. The growth faulting and related flow of salt probably began in Jurassic time, as is indicated by increasing offsets seen in deep strata. Both faulting and diapirism seem to still be active, because strata near the sea bottom are offset at the fault and disturbed sea floor is associated with salt flow.

6. Only the Carolina Trough and Scotian Basin have widespread salt domes off eastern North America, probably because they were the only basins to accumulate large thicknesses of salt. Basements beneath those two troughs also seem to be thinner than those beneath other basins, probably due to greater thinning by stretching during the rifting phase. This may have resulted in greater early subsidence of the Carolina Trough and Scotian Basin and, thus, in more time to accumulate salt.

ACKNOWLEDGMENTS

Mahlon M. Ball and John S. Schlee reviewed this manuscript and offered valuable suggestions. We thank Margaret Clare Mons-Wengler for preparing the manuscript and Patricia Forrestel and Jeffrey Zwinakis for their drafting assistance.

REFERENCES CITED

- Amato, R. V., and E. K. Simonis, 1980, Geologic and operational summary, cost No. G-2 well, Georges Bank area, North Atlantic OCS: U.S. Geological Survey Open-File Report 80-269, 116 pp., 3 plates.
- Aymé, J. M., 1965, The Senegal salt basin *in* Salt Basins around Africa: Elsevier, Amsterdam, The Institute of Petroleum, p. 83-90.
- Ball, M. M., R. M. Gaudet and G. Leist, 1968, Sparker reflection seismic measurements in Exuma Sound, Bahamas (Abs); American Geophysical Union, Transcripts v. 49, p. 196-197.
- Bishop, W. F., 1973, Late Jurassic contemporaneous faults in north Louisiana and south Arkansas: AAPG Bulletin, V. 57, p. 858-877.
- Bruce, C. H., 1973, Pressured shale and related sediment deformation — mechanism for development of regional contemporaneous faults: AAPG Bulletin, v. 57, p. 878-886.
- Burke, Kevin, 1975, Atlantic evaporates formed by evaporation of water spilled from Pacific Tethyan and southern oceans: *Geology*, v. 3, p. 613-616.
- Cloos, Ernst, 1968, Experimental analysis of Gulf Coast fracture patterns: AAPG Bulletin, v. 52, p. 420-444.
- Crans, W., and G. Mandl, 1981a, On the theory of growth faulting, part II (b) — genesis of the "unit": *Journal of Petroleum Geology*, v. 3, p. 333-355.
- , and —, 1981b, On the theory of growth faulting, Part II (c) — genesis of the "unit": *Journal of Petroleum Geology*, v. 3, p. 455-576.
- Dillon, W. P., J. A. Grow, and C. K. Paull, 1980, Unconventional gas hydrate seals may trap gas off southeast U. S.: *Oil and Gas Journal*, v. 78, no. 1, p. 124, 126, 129, 130.
- Edwards, M. B., 1976, Growth faults in Upper Triassic deltaic sediments, Svalbard: AAPG Bulletin, v. 60, p. 341-355.
- , 1981, Upper Wilcox Rosita delta system of south Texas — Growth-faulted shelf-edge deltas: AAPG Bulletin, v. 65, p. 54-73.
- Evans, Robert, 1978, Origin and significance of evaporates in basins around Atlantic margin: AAPG Bulletin, v. 62, p. 223-234.
- Falvey, D. A., 1974, The development of continental margins in plate tectonic theory: *Australian Petroleum Exploration Association Journal*, v. 14, p. 95-106.
- Grow, J. A., 1980, Deep structure and evolution of the Baltimore Canyon Trough in the vicinity of the COST No. B-3 well, *in* I? A. Scholle, ed., *Geological studies of the COST No. B-3 well, United States mid-Atlantic continental slope area U.S. Geological Survey Circular 833*, p. 117-132.
- , R. E. Mattick, and J. S. Schlee, 1979, Multi-channel seismic depth sections and interval velocities over outer continental shelf and upper continental slope between Cape Hatteras and Cape Cod, *in* J. S. Watkins, Lucien Montadert, and I? W. Dickerson, eds., *Geological and geophysical investigations of continental margins: AAPG Memoir 29*, p. 65-83.
- Grunau, H. R., et al, 1975, New radiometric ages and seismic data from Fuerteventura (Canary Islands), Maio (Cape Verde Islands), and São Tomé (Gulf of Guinea), *in* *Progress in geodynamics: North-Holland, Amsterdam, Geodynamics Scientific Report #13*, p. 90-110.
- Hardin, F. R., and G. C. Hardin Jr., 1961, Contemporaneous normal faults of Gulf Coast and their relation to flexures: AAPG Bulletin, v. 45, p. 238-248.
- Harding, T. I?, and J. D. Lowell, 1979, Structural styles, their plate tectonic habitats, and hydrocarbon traps in petroleum provinces: AAPG Bulletin, v. 63, p. 1016-1058.
- Hinz, Karl, 1977, Bericht über den Fahrtabschnitt M 46/1, Hamburg-Casablanca, 8.10.77-5.11.77, der METEOR — Westafrikafahrt 1977: Bundesanstalt für Geowissen-

- schaften und Rohstoffe. Archiv — Nn. 78906, 40 p.
- Hospers, J., and J. Holtke, 1980, Salt tectonics in block 8/8 of the Norwegian sector of the North Sea: *Tectonophysics*, v. 68, p. 257-282.
- Humphris, C. C. Jr., 1979, Salt movement on continental slope, northern Gulf of Mexico: *AAPG Bulletin*, v. 63, p. 782-798.
- Jansa, L. F., J. P. Bujak, and G. L. Williams, 1980, Upper Triassic salt deposits of the western North Atlantic: *Canadian Journal of Earth Sciences*, v. 17, p. 547-559.
- Jansa, L. F., and J. A. Wade, 1975, Geology of the continental margin off Nova Scotia and Newfoundland, in W. J. M. van der Linden, and J. A. Wade, eds., *Offshore geology of eastern Canada*, v. 2, *Regional geology: Geological Survey of Canada, Paper 74-30*, 51-105.
- Keen, C. K., et al, 1975, Some aspects of the ocean-continent transition at the continental margin of eastern North America, in W. J. M. van der Linden, and J. M. Wade, eds., *Offshore geology of eastern Canada*, v. 2, *Regional geology: Geological Survey of Canada, Paper 74-30*, p. 189-197.
- Kent, K. M., J. A. Grow, and W. P. Dillon, 1979, Gravity studies of the continental margin off northern Florida: *Geological Society of America, Abstracts with Programs*, v. 11, no. 4, p. 184.
- Klitgord, K. D., and J. C. Behrendt, 1979, Basin structure of the U.S. Atlantic Continental Margin, in J. S. Watkins, L. Montadert, and P. W. Dickerson, eds., *Geological and geophysical investigations of continental margins: AAPG Memoir 29*, p. 85-112.
- Lehner, Peter, 1969, Salt tectonics and Pleistocene stratigraphy on continental slope of northern Gulf of Mexico: *AAPG Bulletin*, v. 53, p. 2431-2479.
- McPherson, B. A., 1978, Sedimentation and trapping mechanism in Upper Miocene Stevens and older turbidite fans of southeastern San Joaquin Valley, California: *AAPG Bulletin*, v. 62, p. 2243-2274.
- Ocamb, R. D., 1961, Growth faults of south Louisiana: *Transactions of the Gulf Coast Association of Geological Societies*, v. 11, p. 139-175.
- Parker, T. J., and A. N. McDowell, 1955, Model studies of salt-dome tectonics: *AAPG Bulletin*, v. 39, p. 2384-2470.
- Paul, C. K., and W. P. Dillon, 1981, Appearance and distribution of the gas hydrate reflection in the Blake Ridge region, offshore southeastern United States: *U.S. Geological Survey Miscellaneous Field Studies Map, MF 1252*.
- Quarles, Miller, Jr., 1953, Salt-ridge hypothesis on origin of Texas Gulf Coast type of faulting: *AAPG Bulletin*, v. 37, p. 489-508.
- Rider, M. H., 1978, Growth faults in Carboniferous of western Ireland: *AAPG Bulletin*, v. 62, p. 2191-2213.
- Seglund, J. A., 1974, Collapse-fault systems of Louisiana Gulf Coast: *AAPG Bulletin*, v. 58, p. 2389-2397.
- Shiple, T. H., et al, 1979, Seismic evidence for widespread possible gas hydrate horizons on continental slopes and rises: *AAPG Bulletin*, v. 63, p. 2204-2213.
- Short, K. C., and A. J. Stäuble, 1967, Outline of geology of Niger delta: *AAPG Bulletin*, v. 51, p. 761-779.
- Sylwester, R. E., W. P. Dillon, and J. A. Grow, 1979, Active growth fault on seaward edge of Blake Plateau, in Gill, Dan and D. F. Merriam, eds., *Geomathematical and Petrophysical Studies in Sedimentology: Oxford, Pergamon Press*, p. 197-209.
- Tator, B. A., and L. E. Hatfield, 1975, Bahamas present complex geology: *Oil and Gas Journal*, Part 1, v. 73, No. 43, p. 172-176; Part 2, v. 73, No. 44, p. 120-122.
- Templeton, R. S. M., 1970, The geology of the continental margin between Dakar and Cape Palmas, in *The geology of the east Atlantic continental margin*, 4, Africa: United Kingdom, Institute of Geological Sciences Report No. 70/16, p. 47-60.
- Tucholke, B. E., 1979, Relationship between acoustic stratigraphy and lithostratigraphy in the western North Atlantic Basin in Tucholke et al, eds., *Initial reports of the deep sea drilling project*, v. 43, Washington, D. C., U.S. Government Printing Office, p. 827-846.
- Uchupi, Elazar, and J. A. Austin, 1979, The geologic history of the passive margin off New England and the Canadian Maritime Provinces: *Tectonophysics*, v. 59, p. 53-69.
- Weimer, R. J., and T. L. Davis, 1977, Stratigraphic and seismic evidence for Late Cretaceous growth faulting, Denver Basin, in C. E. Payton, ed., *AAPG Memoir 26*, p. 277-299.